RSC Sustainability

ROYAL SOCIETY OF CHEMISTRY

CRITICAL REVIEW

View Article Online
View Journal | View Issue

Cite this: *RSC Sustainability*, 2025, **3**, 2079

Photocatalytic valorisation of real-world substrates

Kathryn Ralphs, *[a] Junhong Liu,[a] Lan Lan,[b] Christopher Hardacre,[b] Nathan Skillen[c] and Peter K. J. Robertson[a]

There are several key environmental sustainability challenges that the world needs to address over the next thirty years, particularly against the backdrop of achieving global net carbon zero emission this century. In addition to reducing global carbon emissions, the provision of clean "green" energy, reduction of water pollution and production of high value chemicals in a sustainable manner are clear priorities for sustainable economic growth. The photocatalytic valorisation of real-world substrates (waste biomass, plastic pollution and wastewater) is an opportunity to contribute significantly towards tackling water pollution, cutting CO_2 emissions and contributing to sustainably producing value added chemicals and hydrogen from waste materials and water contaminants/pollutants. To date, however, research is critically lagging in terms of the utilization of actual real-world substrates and instead concentrates on much simpler model compounds such as sugars, monomers, dyes and individual pollutants. Lack of progress in this field is further exacerbated by the general lack of scaling up of photocatalytic technology. Nevertheless, there are some pioneers who have explored the photocatalytic valorization of real-world waste materials which have been highlighted in this review. This review considers the application of semiconductor photocatalysis for such applications with a particular focus on valorisation of waste biomass (*e.g.* cardboard, grass, wood), plastic pollution (*e.g.* plastic bottles) and wastewater effluents (*e.g.* from juice processing factories) to produce hydrogen and value-added chemicals. Current engineering aspects are reviewed and discussed. A perspective of the role of photocatalysis in the circular economy is also discussed and an overall perspective and future outlook is presented.

Received 15th October 2024
Accepted 12th March 2025

DOI: 10.1039/d4su00646a

rsc.li/rscsus

Sustainability spotlight

Transitioning to a net carbon zero world is a monumental task for humankind. It is a very complex multifaceted ambition that requires substantial innovation and investment. The hydrogen economy is considered to be one of the most promising options to decarbonise the energy and transport sectors. The circular economy can also play a major role in reaching net zero and reducing carbon emissions. Therefore, this review has been prepared to assess the potential of the photocatalytic valorization of real-world waste products such as food waste, wastewater and plastic pollution to generate value added chemicals and hydrogen. The research detailed in the review clearly aligns with SDG7, SDG12 and SDG13.

1. Introduction

1.1 Current state of play

It is indisputable that human activity has had a devastating impact on the planet. Human activity results in around 51 billion tonnes of greenhouse gases added to the atmosphere every year.[1] From fossil fuel use alone, we emit over 34 billion tonnes of CO_2 per year,[2] burn 929 million tonnes of coal each year,[3] consume 94 million barrels of oil per day, and mine 1.3 million tonnes of precious metals, 207 million tons of industrial metals and over 3 billion tonnes of iron ore per year.[4] Each year our plastic production rises with just under 460 million tonnes of plastic being produced in 2019.[5] It is estimated we cut down 10 million hectares of forest per year,[6] the size of animal populations for which data is available has declined by 69% from 1970.[7] Since the rise of humans, wild mammals have declined by 85%.[8] Livestock activities contribute 18% (made up of 9% total CO_2, 34% CH_4 and 65% NO_x) of the total greenhouse gas emissions, which is more than the road transport sector.[9]

With an ever-increasing global population, the catastrophic costs for the planet are only going to worsen. Population is the multiplier to everything we as humans consume and the damage we do to the planet.[10,11] On 15th November 2022 the world's population reached 8 billion people. By 2050 it is projected to reach 8.5 billion and to increase further to 9.7 billion in 2050. By 2100 the UN estimates the global population will reach 10.4 billion people.[12] Population and economic growth

[a]*School of Chemistry and Chemical Engineering, Queen's University Belfast, Belfast, BT95AG, UK. E-mail: k.ralphs@qub.ac.uk*

[b]*Department of Chemical Engineering, School of Engineering, The University of Manchester, Manchester, M139PL, UK*

[c]*International Centre for Brewing & Distilling, School of Engineering and Physical Sciences, Heriot Watt University, Edinburgh, EH144AS, Scotland*

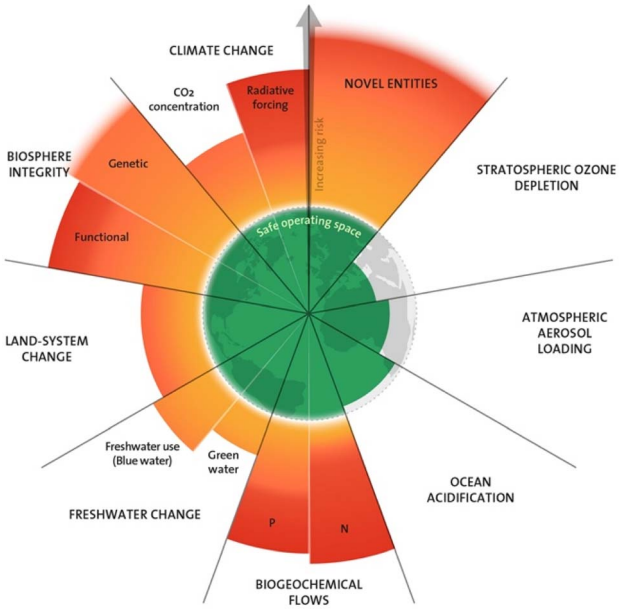

Fig. 1 The 2023 planetary boundaries. Reproduced from Stockholm Resilience centre, based on analysis in ref. 23. Licensed under CC BY-NC-ND 3.0. Credit: "Azote for Stockholm Resilience Centre".

are the driving factors towards increased greenhouse gas emissions.[13–20] Despite the evidence,[21] however, this is often overlooked by policy makers.

The planetary boundaries framework[22] is based upon Earth system science and identifies boundaries that are vital for maintaining the stability and resilience of the planet. As of 2023 nine boundaries have been identified and currently all nine are heavily negatively affected by human activity (Fig. 1).[23] According to the framework, transgressing these boundaries will increase the risk of irreversible climate change with consequences that are detrimental or even catastrophic for large parts of the world.

The effects of climate change are ubiquitous and impossible to ignore. Earth's temperature has risen by an average of 0.08 °C per decade since 1880. Since 1981 the rate of warming has more than doubled to 0.18 °C per decade (Fig. 2). The 10 warmest years since recording began, have occurred since 2010. In 2022 the surface temperature was 1.06 °C warmer than the pre-industrial period (1880–1900).[27] This rapidly increasing warming of the Earth's surface has a myriad of cataclysmic consequences. The ice sheets are melting,[28] sea levels are rising,[29] and oceans are becoming more acidic.[30] Forest fires are increasing in occurrence and ferocity,[31,32] rainfall patterns are shifting, leading to flooding[33] and droughts,[34] biodiversity is being lost,[35] and food[36] and water security[37] is being threatened. Ultimately more of the world's population will find themselves living in various types of hostile environments.

1.2 Net zero

Net zero, the new buzz word of recent times, was first popularized by the Paris Agreement 2015 to limit the impact of

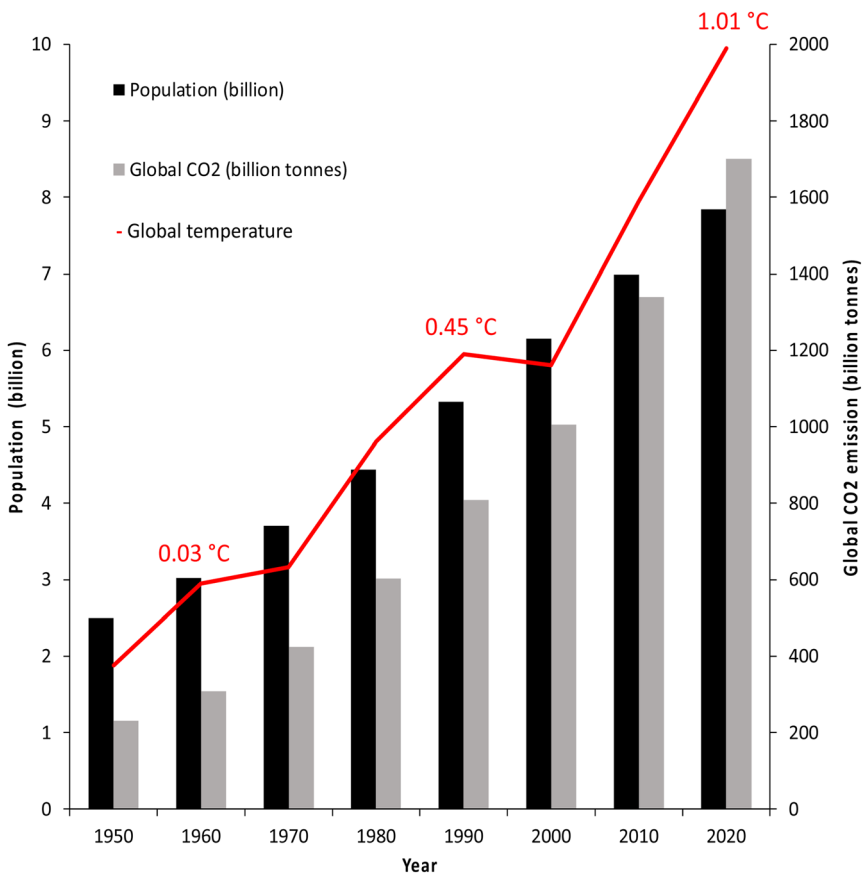

Fig. 2 Graph showing global CO_2 emissions,[24] world population[25] and global temperature with respect to 20th century average temperature.[26]

greenhouse gas emissions.[38] The United Nations definition of net zero is "cutting greenhouse gas emissions to as close to zero as possible with any remaining emissions reabsorbed from the atmosphere by oceans and forests for instance".

Net zero has been met with enthusiasm around the globe with a growing coalition of countries, business and other institutes pledging to net zero emissions. More than 70 countries, including China, US and EU have set net zero targets. In 2019, the UK was one of the first major economies to pass laws that aligned with these targets by requiring all greenhouse gas emissions to be net zero (in comparison to levels in 1990) by 2050.[39,40]

The Paris Agreement is a binding agreement that brings all nations together to combat climate control with the aim of keeping the increase in the global average temperature below 2 °C (above pre-industrial levels). More recently IPCC has stressed that the average global temperature increase must be kept below a 1.5 °C rise to prevent devastating climate related consequences. To achieve this 1.5 °C goal, the UN climate science panel have stated that global CO_2 emissions must fall by 43% by 2030, and to net zero by 2050.[41]

Net zero is a very ambitious target and is an excellent idea in theory to alleviate CO_2 levels; however in practice it could possibly end up being nothing more than *Schlimmbesserung*, by depending on the use of carbon offsets to reach net zero targets. Carbon offsets are tradable "rights" or certificates linked to activities that lower the amount of CO_2 in the atmosphere.[42] Carbon offsets are widely used by individuals, corporations, and governments to mitigate their greenhouse gas emissions on the assumption that offsets reflect equivalent climate benefits achieved elsewhere. By purchasing carbon credits, a person/company can pay to have their carbon emissions offset rather than taking any actions to lower their emissions. Unfortunately, many countries are yet to set out detailed plans to achieve their net zero pledges and are opaque about the role of carbon offsetting. The Paris Agreement left it up to each country to define their own emissions pathways and their plans to contribute to global net zero. There is no official method to quantify the adequacy, ambition, or fairness of a country's global net zero contributions.[43]

Net zero, done right, is an extremely ambitious and not a straightforward target to achieve. It is becoming evident, however, that net zero is probably almost certainly not enough by itself to prevent global temperatures increasing beyond the limits set out in the Paris Agreement.[44] Nevertheless, in order to achieve or come to close to achieving net zero, a rapid global transformation with huge investment is needed. It is estimated $125 trillion of climate investment is needed by 2050 to meet net zero.[45] In 2020 the UK government set out a 10-point plan to accelerate the UK's path to net zero.[46] The plan is to mobilise £12 billion of government investment, and potentially 3 times as much from the private sector, to create and support up to 250 000 green jobs. The 10-point plan focuses on low carbon hydrogen, offshore wind, nuclear power, zero emission vehicles and carbon capture as well as protecting the environment, working towards "jet zero", greener buildings and green public transport.[47]

1.3 Hydrogen

Green hydrogen, *i.e.*, hydrogen produced *via* water electrolysis using renewable electricity, is thought to be one of the most promising options to decarbonize the energy and transport sector.[48,49] Hydrogen is largely regarded as a potential clean, cost effective, reliable, and potentially sustainable energy vector. "Energy vector" refers to "an energy-rich substance that facilitates the translocation and/or the storage of energy with the intention of using it at a distance in time and/or space from the primary production site.[50] Hydrogen is not a primary energy source but an energy carrier, like electricity.[51] Energy obtained from renewable sources, such as solar, wind and wave can be stored as chemical potential energy in hydrogen and hydrogen-rich materials (ammonia, urea, formate, *etc.*) and liberated by oxidation, generating water as the by-product. It is also possible to produce sustainable hydrogen through photocatalysis using renewable sources such as biomass or waste streams which is discussed in Section 2.

Hydrogen is the lightest element and the most abundant gas in the universe. Despite the abundance of hydrogen, obtaining this molecule in its elemental form is not facile. Industrially, hydrogen is produced *via* hydrocarbon reforming and pyrolysis. Steam reforming of methane is the most widely used method for large scale hydrogen production and has a conversion efficiency between 74 and 85%. Steam and natural gas are reacted over a nickel catalyst at temperatures of 850–900 °C (grey hydrogen). It is estimated this method produces 0.3–0.4 m^3 CO_2 per m^3 H_2.[52] By 2021, 47% of the global hydrogen production was obtained from natural gas, 27% from coal, 22% from oil and 4% from electrolysis.[53]

Despite the immense potential of green hydrogen to decarbonize the world's economy, the economics are challenging.[54] The cost of producing green hydrogen varies widely by location and availability of renewable resources. For example, in parts of the Middle East, green hydrogen can be produced for 3–5 euro per kg. However, in Europe, the cost of production can vary from 3–8 euro per kg.[55] In the USA, grey hydrogen costs just $2 per kg due to the low cost of fracked natural gas, while due to increasing natural gas prices in Europe because of the ongoing war in Ukraine, the cost to produce grey hydrogen is $6–8 per kg.[56] With grey hydrogen now costing more than green hydrogen in some regions, this could significantly accelerate the ramping up of the hydrogen economy.[57] It is estimated that by 2030 a UK-wide hydrogen economy could be worth £900 million and create over 9000 high quality jobs. By 2050 this is estimated to increase to 100 000 jobs and a hydrogen economy worth up to £13 billion.[58] In addition, modelling data suggests that 41 Mt of CO_2e could be saved between 2023 and 2032 as a result.[59]

As well as use as an energy vector, hydrogen as a replacement for fossil fuels is a significant component of many decarbonization strategies.[60] Hydrogen can be utilized as a fuel either *via* combustion or an electrochemical fuel cell. A fuel cell generates electricity from hydrogen with only water as the by-product. It is assumed, however, in the UK that most hydrogen will be utilized as a fuel by combustion. Hydrogen is already blended

into streams of natural gas across the globe.[61–64] However, one of the major issues of combusting hydrogen, which is frequently overlooked, is that it can lead to the formation of NO_x at a higher quantity than produced by the combustion of fossil fuels.[65,66] Another area of concern is the transport and storage of hydrogen. If steel is exposed to hydrogen at high temperatures, it can cause the steel to become brittle resulting in leaks and subsequent explosions. Consequently, current infrastructure cannot be used to store and transport hydrogen. Significant investment is required to upgrade current infrastructure to utilize hydrogen as fuel.

1.4 Photocatalysis

Photocatalysis harnesses light energy using a semiconductor material *i.e.*, a photocatalyst, to drive chemical reactions. Upon the absorption of light of an appropriate wavelength an electron hole pair is generated, in which initially the photogenerated hole is created in the valence band and the photogenerated electron is located in the conduction band. The difference in energy between the two bands is called a band gap and the light energy absorbed must be equal to or greater than this band gap in order to promote the electron.[67] The generation of an electron hole pair initiates a series of complex processes and mechanisms that yield oxidized and reduced species.[68] Photogenerated electrons can react with oxygen to form a superoxide radical. The photogenerated holes can be transferred to the target molecule leading to its oxidation or can react with water to generate hydroxyl radicals. These hydroxyl radicals can then go on to oxidize the target molecules. The actual mechanism is very complex and not easy to elucidate. Numerous publications have discussed the mechanism in detail and can be found elsewhere.[69–74] A simplified summary of the potential mechanism is given in Fig. 3.

Photocatalysis holds significant importance due to its potential to address various environmental and energy challenges. It is an extremely active and constantly developing research area ranging from pollution degradation,[75,76] water electrolysis for clean hydrogen production,[77] solar energy conversion,[78] water[79] and air purification,[80] development of photonic materials and devices and sustainable chemistry and synthesis and energy.[81]

Semiconductor photocatalysis is clearly a very versatile technology that could have huge potential scope in providing a route to low carbon fuels such as hydrogen *via* reduction of protons by conduction band electrons. A further potential advantage of this process is that the corresponding valence band oxidation reaction can be simultaneously used for other environmentally beneficial processes such as water treatment or for generation of high value chemicals through oxidation of waste materials such as microplastics or cellulosic biomass. This review considers the utilisation of photocatalysis as a process for the valorisation of a range of such "real-world substrates" and considers the potential of this process as part of future circular economy and net carbon zero energy and chemical production. Specifically, examples of real-life substrates which are considered in this review include biomass, waste plastics and contaminated wastewater.

2. Substrates

2.1 Biomass

More recently photocatalytic reforming of biomass has become one of the most rapidly evolving applications in the field with enormous potential to contribute to a more sustainable circular economy.[82–84] Biomass can be converted by use of a suitable semiconductor photocatalyst and light energy, generating value added chemicals, sustainable hydrogen and fuels. The first report of biomass reforming *via* photocatalysis was by Kawai and Sakata in 1980;[85] however it is only in the last decade that publications in this area have begun to increase, which is thought to be due to the expansion of the bioenergy sector and the demand for sustainable hydrogen production. The concept of a biorefinery focuses on the use of biomass in place of fossil fuels[86] to generate both bioenergy, value-added chemicals and

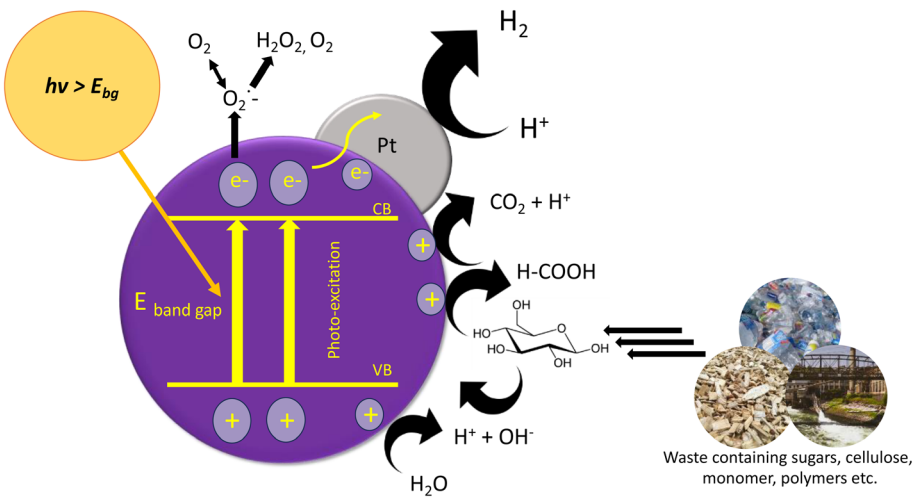

Fig. 3 Simplified figure showing a potential photocatalytic mechanism.

green hydrogen. The integration of the photocatalytic reforming of biomass with the biorefinery concept and the bioenergy sector holds much promise for advancing a sustainable society and contributes vastly to a decarbonized economy.[87]

As the largest biomass energy resource, lignocellulosic biomass, which is the major component of trees, grasses, and straws, has drawn considerable attention in recent years. Lignocellulose is a functionalized biopolymer consisting of three major components, which are lignin (25–30%), cellulose (40–45%) and hemicellulose (30–35%)[88] (Fig. 4). Cellulose and hemicellulose, also known as polysaccharides, are biopolymers composed of β-D-glucose and C5, C6 sugars and sugar acids respectively. These units are linked by β-1,4-glycosidic bonds and their degrees of polymerization can reach 800 to 10 000.[89] Compared to the components above, lignin, the largest natural large scale of aromatic sources,[90] is a complicated three-dimensional amorphous polymer, consisting of three aromatic main units: syringyl, guaiacyl, and *p*-hydroxyphenyl units, as well as other molecules.[91] As these main units all contain a phenyl and a propyl side chain, the typical aromatic unit in lignin is generally referred to as the phenyl propane unit (ppu). The number of methoxyl groups varies from unit to unit, with sinapyl containing two methoxy groups, coniferyl alcohol with one, and *p*-coumaryl alcohol with none. Also, the amount of each unit in lignin is related to the plant species. For instance, the lignin of softwoods has a high content of guaiacyl monomers, that of hardwoods is a mixture of guaiacyl and syringyl, and that of grasses presents a mixture of all three monomers.[92]

The utilization of biomass for bioenergy production can have negative repercussions on food security. Providing adequate food and nutrition to an increasing population while conserving natural resources is a key aspect of the United Nations sustainable development goals.[93] Globally, two billion people have nutritional deficiencies and around 800 million still suffer from hunger.[94] A recent review of the literature found that 56% of studies on the effects of bioenergy on edible and inedible feedstocks reported a negative impact on food security regardless of feedstock source. It is vital to maintain food security while expanding the bioenergy sector. One way to do this is to utilize waste as a feedstock for bioenergy/chemicals/sustainable hydrogen production.[95] Agricultural residues account for 21% of the total biomass resources and are associated with manure from livestock, vegetable/fruit waste[96] and lignocellulosic biomass such as rice straw, wheat straw, maize straw, *etc.*[97,98] Nevertheless, these resources are ineffectively utilized, whereby 75% of straw is combusted or dumped and only 0.5% is used for biogas production.[99]

Biomass such as agricultural residues and waste, plastics, sludge and industrial effluent are the most viable options of waste streams for energy production and valorisation *via* photocatalysis. Each feedstock will be discussed in detail in this review. There are numerous benefits to employing waste as a feedstock; for example, agricultural waste is renewable and abundant while using plastic waste as a feedstock can offer a potential solution to waste management and adding value to waste materials. However, until recently the majority of research has focused on the photocatalytic conversion of simple molecules, such as glucose[100] or cellulose[101–103] as well as cleavage of β-O-4 ether bonds found in lignin using model lignin compounds.[104,105] However more recently vast progress has been made in using much more complex lignin model compounds.[106,107] It is imperative that research using real-world substrates as well as reactor design and scale up is radically ramped up. The Technology Readiness Level (TRL) of photocatalysis techniques needs to be at a much higher level to reach

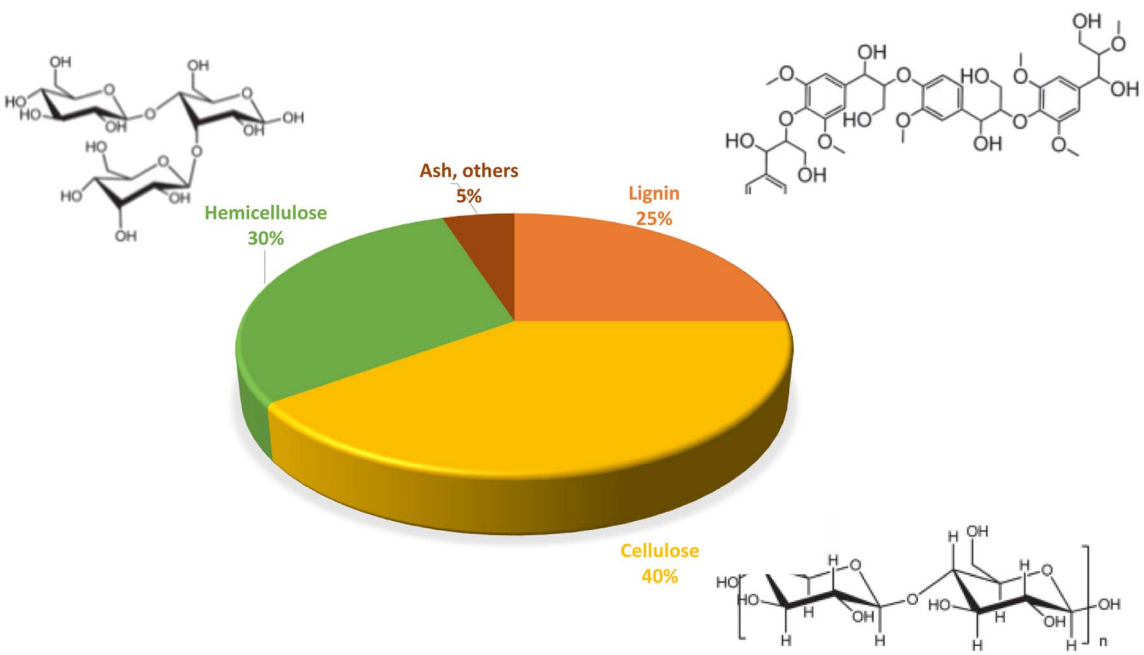

Fig. 4 Proportion of hemicellulose (30–35%), cellulose (40–45%) and lignin (25–30%) as lignocellulose components.

its full potential. This review aims to analyse the current state of research and provide a prospective moving forward with respect to utilizing real word feedstocks as photocatalytic substrates and potential future technology barriers as the field develops. In the following section, the photocatalytic valorisation of real-world lignocellulosic biomass feedstocks will be discussed. In context these reports will be classified by products such as hydrogen and value-added chemicals such as formic acid, hydrocarbons, and aldehydes.

2.1.1 Biomass for hydrogen evolution. Green hydrogen generated by photocatalytic water splitting has emerged as a promising alternative to fossil fuels.[108] So far, the photocatalytic hydrogen production is limited by the high overpotential of the oxygen evolution reaction (OER, $\Delta E^0 = -1.23$ V). To improve the quantum yield of hydrogen production from water splitting, biomass and its derivatives are used as sacrificial agents to overcome the high oxidation overpotential, namely by biomass photoreforming. The following section provides more details about hydrogen production from biomass.

In 1980, Sakata *et al.*[109] utilized various types of biomasses as substrates to test their feasibility for photocatalytic hydrogen production, including cherry wood, Dutch clover, golden-rod, water hyacinth and rice plant. Using a 4% Pt/TiO_2 photocatalyst, up to 54 μmol of hydrogen was produced after 10 h irradiation under a 500 W Xe lamp from Dutch clover. The hydrogen yields under the same conditions ranged from 12 to 25 μmol for the other biomass feedstocks. It's worth noting that each of the feedstocks displayed 2–7 times higher hydrogen yield following pre-treatment with 10 M NaOH.

Speltini *et al.*[110] also utilized a Pt/TiO_2, with a Pt loading of 0.5%, catalyst for solar photocatalytic hydrogen production from water suspended cellulose (CLS). It was reported that under 366 nm (UV-A) irradiation, CLS greatly enhanced water splitting, with yields up to ten-fold higher than those observed in neat water. At the same time 5-hydroxymethylfurfural (HMF) was identified as the result of polysaccharide depolymerization. Encouraged by this result, rice husk and alfalfa (*Medicago sativa*) stems as raw cellulosic biomass were evaluated, with reaction yields threefold higher than those observed in the water splitting process in pure water.

In other research,[111] 2% Pt/TiO_2 was utilized in photoreforming of alkali-pre-treated bamboo, rice straw, and silver grass saccharification and fermentation solution. The transformation was reported in three steps. The first step started with treatment with NaOH solution at 95 °C for 1 h. Subsequently, the pre-treated lignocellulose was converted into a suspension of ethanol and xylose, xylanase, and *S. cerevisiae* by a simultaneous saccharification and fermentation process (SSF) using cellulase and xylanase in acetate buffer at 34 °C. The yeast suspension converted cellulose to ethanol and xylose. The xylose was subsequently photoreformed to ethanol and hydrogen using a Pt/TiO_2 photocatalyst. The hydrogen yield demonstrated a combustion energy of 73.4–91.1% compared to that of the alkali-pre-treated lignocelluloses (holocellulose).

Over a 1% Pt/TiO_2 photocatalyst, alkaline pre-treated corn stover and its waste liquid produced 212.3 and 205.4 μmol g_{cat}^{-1} h^{-1} H_2, respectively, under the irradiation of a 300 W Xe lamp.[112] The concentration of NaOH and pre-treatment temperature were found to greatly influence H_2 production. Alkali treatment on corn stover resulted in changes in morphology, structural composition, and functional groups due to the removal of lignin and hemicellulose.[113] The measured and calculated crystallinity (CrI) of corn stover increased from 39.04% to 51.06% after alkali treatment, which was attributed to the partial removal of hemicellulose and lignin under alkaline conditions, dissociation of hydrogen bonds between lignin, hemicellulose and cellulose, and destruction of amorphous cellulose due to swelling. Hydrogen production increased sequentially after the alkaline pre-treatment process. When fescue grass was used as a substrate[114], after washing with water and then methanol at 55 °C and then drying in an oven at 120 °C overnight, 0.6 ml hydrogen was generated following irradiation in the presence of a Pt/TiO_2 photocatalyst. Jaswal *et al.* investigated dilute acid hydrolysis of pinewood for the production of hydrogen using a 1% Pt/TiO_2 catalyst and activated carbon treatment. After 8 consecutive photocatalytic cycles of activated carbon/acid treated material a cumulative yield of 19.9 ml H_2 per h pinewood was achieved.[115]

The use of photocatalysts such as TiO_2 modified with precious metals for H_2 production from biomass is well documented as detailed above. The use of precious metals, however, increases the cost, and cheaper alternatives need to be developed for the photocatalytic biomass conversion process. The following reports of photocatalysts developed for hydrogen production were reviewed.

Cu, In doped ZnS derived from ZIF-8 showed high activity in biomass photoreforming for hydrogen production.[116] Grass, paper and wood were chosen as real-world substrates. Under simulated solar (Air Mass 1.5 spectrum, AM 1.5) irradiation in 10 M NaOH solution at 70 °C, 31.7, 60.2 and 73.9 μmol per h per g H_2 were produced respectively. To investigate the contribution of various components of biomass to hydrogen production, model reagents such as glucose, cellobiose, formate, and cellulose were tested for hydrogen production respectively. Notably the hydrogen production rate was low when lignin was used as substrate, which indicates that most of the generated hydrogen was contributed by the cellulosic portion of raw biomass.

Thermal radiative Pt/SiC/CdS[117] performed well as a material for the photocatalytic generation of hydrogen from biomass. In an alkaline pre-treated grass solution (10 M NaOH), 259 μmol per h per g H_2 yield was achieved under irradiation with a 300 W Xe lamp light source at 343 K. In addition to grass, wood and paper were also used as raw biomass to investigate the efficiency of hydrogen production under this catalyst. The hydrogen production yield decreased in the order of grass, wood and paper, which was not further investigated in this work.

Typical non-metal photocatalyst carbon nitride (CN_x) was also investigated. Kasap *et al.*[118] reported cyanamide-functionalized carbon nitride ($^{NCN}CN_x$) allowed visible light-driven photoreforming of raw biomass. All of the raw biomass examined, including sawdust, paper, cardboard, bagasse and wooden branches, successfully resulted in H_2 formation.

Sawdust produced 202 μmol h^{-1} g^{-1} with NiP and $^{NCN}CN_x$ materials under simulated solar light (AM 1.5 G, 100 mW cm^{-2}). It is noteworthy that lignin and its components were generally poor at producing hydrogen under these conditions.

In addition to raw biomass, raw biomass waste was also used as a substrate for hydrogen production. Pulp and black liquor, as one of the most abundant fibrous biomass wastes, has great potential to be used as a substrate for hydrogen production. The pulp and paper industry ranks sixth among the world's most polluting industries, creating toxic wastewater on a large scale after the paper is processed.[119] Pulp and paper are manufactured from cellulose fibres and other plant materials. During the manufacturing process, deposits of cellulose, lignin, phenols, fatty acids, tannins, and resins are released from the pulp to form an alkaline, sticky, dark black waste called black liquor. The production of pulp and paper generates large quantities of pollutants, mainly in the form of high concentrations of suspended solids (SS), chemical oxygen demand (COD), toxicity and biochemical oxygen demand (BOD).[120] Toxic effects on various fish species due to exposure to pulp and paper mill effluents have been reported.[121–125] Therefore, the oxidative degradation of lignocellulosic biomass from waste pulp and black liquor with simultaneous hydrogen production is an attractive research direction.

Zhong *et al.*[126] designed and synthesized a three-dimensional ordered macroporous (3DOM) structure TiO_2–Au–CdS for biomass photoreforming for hydrogen production (Fig. 5). Cellulose, cellobiose and dissolved pulp were tested. As the complexity of structures grew, the hydrogen production rates gradually decreased from 273.9 μmol h^{-1} g^{-1} (cellobiose) to 79.7 μmol h^{-1} g^{-1} (dissolved pulp). It is worth noting that other gaseous components such as CO and CH_4 were also produced as part of the photocatalytic process.

Zou *et al.*[127] combined photoreforming and acid hydrolysis to achieve simultaneous biomass conversion and hydrogen production. Paper pulp as a representative raw feedstock resulted in 89% H_2 yields, based on the number of monosaccharides in pulp. At 403 K the efficient and stable hydrogen generation could reach 1320 μmol per h per g cat. in 0.6 M H_2SO_4. The products of the pulp conversion were, however, not described.

In addition to the paper industry, waste and wastewater in the food industry are also potential hydrogen-producing biomass waste. Low-toxicity food industry wastewater usually contains high concentrations of organic matter (*e.g.*, sugars, proteins, *etc.*).[128] Therefore, if it is discharged without treatment, it can easily lead to eutrophication of the water body thus creating an anoxic environment, which ultimately makes it toxic for fish and other aquatic organisms to survive.[129] Organic matter in wastewater can act as a sacrificial and proton donor for oxidative degradation along with hydrogen production[130] and will be discussed in detail in Section 2.3.

2.1.2 Biomass to value added chemicals. In addition to hydrogen production, lignocellulosic biomass valorization is another way to utilize raw biomass. Cellulose and lignin, which are the main components of lignocellulosic biomass, have been converted into high value chemicals including 5-hydroxymethylfurfural,[131] vanillin,[132] formic acid,[133] and 2,5-furandicarboxylic acid.[134] These compounds can be utilized as precursors in the synthesis of commodity chemicals and liquid fuels,[135] flavour compounds in food, beverages, perfumes, and pharmaceuticals,[136] and monomer substitutes for the synthesis of polymers,[134] respectively.

In 1995, Greenbaum *et al.*[137] investigated the photocatalytic conversion of woody biomass to volatile hydrocarbons. It was reported that the wood samples were converted into a wide range of hydrocarbons from C4 to C20 hydrocarbons in a flowing photoreactor over a ZnO photocatalyst irradiated with a Xe lamp. This research demonstrated the feasibility of photoreforming lignocellulosic biomass into value added chemicals.

Nguyen and co-workers reported a photocatalytic method for redox-neutral depolymerization of raw lignin biomass. Raw lignin biomass *i.e.* grand fir, ponderosa, cedar and larch which were extracted from the corresponding sawdust were investigated with $[Ir(dFCF_3ppy)_2$-$(5,5'$-$dCF_3bpy)]PF_6$ (ppy; polypyrrole, bpy; 2,2′-bipyridine) as a catalyst under blue LED irradiation for 24 h.[138] 3,4-Dimethoxybenzaldehyde, vanillin and 4-(2-hydroxyethoxy)-3-methoxybenzaldehyde were detected after

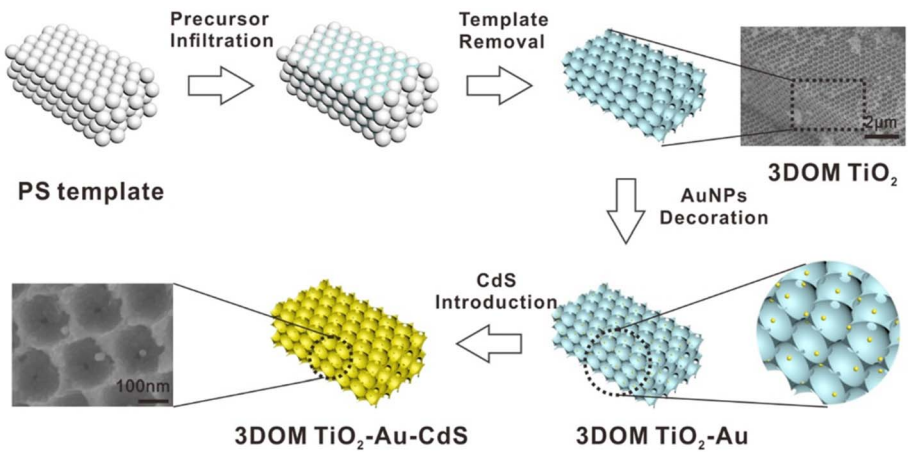

Fig. 5 Schematic illustration of the 3DOM TiO_2–Au–CdS preparation process reproduced from ref. 126 with permission from MDPI.

Table 1 Summary of real-world biomass substrates for photocatalytic valorization

Feedstock details	Catalyst	Experimental conditions	Product details	Reference
Cherry wood Dutch clover Golden-rod Water hyacinth Rice plant Seaweed Algae Oil Cotton Sweet potato	4% Pt/TiO_2	500 W Xe lamp 5 M NaOH pre-treatment	Cotton: 200 μmol H_2 Lignin: 77 μmol H_2 Sweet potato: 378 μmol H_2 Fatty oil: 212 μmol H_2 Cherry wood: 148 μmol H_2 Dutch clover: 142 μmol H_2 Golden rod: 55 μmol H_2 Water hyacinth: 130 μmol H_2 Rice plant: 175 μmol H_2 Chlorella algae: 270 μmol H_2 Seaweed: 166 μmol H_2 Laver seaweed: 332 μmol H_2 Additional products included ammonia, short chain hydrocarbons, ethanol, and methanol	109
Rice husk Alfalfa stems	0.5% Pt/TiO_2	366 nm UV light	Rice husk 18 L H_2 per m^3 under UV-light Rice husk 15 L H_2 per m^3 under natural solar light	110
Bamboo Rice straw Silvergrass	2% Pt/TiO_2	1% NaOH pre-treatment followed by conversion to ethanol and xylose by SSF using enzymes Hg lamp	Bamboo 74% yield H_2 per 10 g bamboo following pre-treatment and SSF Rice straw 96% yield H_2 10 g rice straw following pre-treatment and SSF Silvergrass 97% yield per 10 g silvergrass following pre-treatment and SSF	111
Corn stover	1% Pt/TiO_2	NaOH pre-treatment 300 W Xe lamp	Corn stover: 25.84 μmol per h H_2	112
Fescue grass	0.2% Pt/TiO_2	Grass washed with methanol at 55 °C in an ultrasonic bath then dried overnight 150 W Xe lamp	Fescue grass: 494 μmol per h per g per g_{catal} H_2	114
Grass Wood Paper	Cu and In doped ZnS derived from ZIF-8	No pre-treatment Simulated solar (AM 1.5) irradiation	Grass: 31.7 μmol per h per g H_2 Wood: 73.9 μmol per h per g H_2 Paper: 60.2 μmol per h per g H_2	116
Lignin Grass Wood Paper	0.5% Pt/SiC/CdS	300 W Xe lamp 10 M NaOH reaction media	Lignin: 11 μmol per h per g H_2 Grass: 259 μmol per h per g H_2 Wood: 131.7 μmol per h per g H_2 Paper: 60.7 μmol per h per g H_2	117
Sawdust Paper Cardboard	Activated $^{NCN}CN_x$ and NiP catalyst CN_x was activated by ultra-sonication in a potassium phosphate solution	Solar simulator Xe lamp Reactions carried out in KPi at a pH of 4.5	Sawdust: 202 μmol H_2 per (g CN_x) per h H_2 Paper: 42.7 μmol H_2 per (g CN_x) per h H_2 Cardboard: 46.9 μmol H_2 per (g CN_x) per h H_2	118

Table 1 (*Contd.*)

Feedstock details	Catalyst	Experimental conditions	Product details	Reference
Bagasse Wooden branch			Bagasse: 34.8 μmol H_2 per (g CN_x) per h H_2 Wooden branch: 35.7 μmol H_2 per (g CN_x) per h H_2	
Pulp	3DOM TiO_2–Au–CdS	Pre-treated but not specified how	Pulp: 79.7 H_2 mol per h per g H_2	126
Pine wood	1% Pt/TiO_2	Acid hydrolysis pre-treatment (1% HCL at 180 ° C for 120 min) Xenon lamp AM 1.5 G	Pine wood: 19.9 ml H_2 per g pinewood after 8 consecutive cycles	115
Paper pulp	0.5% Pt/TiO_2	250 W iron doped halide lamp 403 K reaction temperature in acidic reaction media (0.6 M H_2SO_4)	Paper pulp: H_2 1320 μmol per h per g cat.	127
Poplar wood	ZnO	Treatment with either 3 M ferric chloride or nitrate solution or ZnO at 20 000 psi with a lab press	Poplar wood (ferric chloride treated): short chain alcohols, furan, methyl acetate, furfural	137
Pine wood		Canrad-Hanovia compact xenon-cathode tip lamp	Poplar wood (ZnO treated): C4–C20 alcohols, long chain hydrocarbons, aldehydes	
Grand fir	$[Ir(dF(CF_3)ppy)_2(5,5'\text{-}d(CF_3)bpy)]PF_6$	Blue LEDs	Grand fir: 2.1% vanillin, 1.3% 4-(2-hydroxyethoxy)-3-methoxybenzaldehyde. B-Ether bond cleavage: 41%	138
Ponderosa	$PBu_4OP(O)(OtBu)_2$, 3,4-diflurorthiophenol, dioxane		Ponderosa: 2.3% vanillin, 1.4% 4-(2-hydroxyethoxy)-3-methoxybenzaldehyde, B-ether bond cleavage: 34%	
Cedar			Cedar: 3% vanillin, 1.8% 4-(2-hydroxyethoxy)-3-methoxybenzaldehyde, B-ether bond cleavage: 42%	
Larch			Larch: 3.2% vanillin, 1.9% 4-(2-hydroxyethoxy)-3-methoxybenzaldehyde, B-ether bond cleavage: 22%	
Birch woodmeal	Cadmium sulfide quantum dots with MPA ligand (CdS QDs-MPA)	300 W Xe lamp with an ultraviolet (UV) cut-of filter ($\lambda \geq 420$ nm)	Birch woodmeal: syringyl-derived ketones (17.3%) Guaiacyl-derived ketones (7.4%)	139
Rice husk	TiO_2 in aqueous 30% H_2O_2 solution	500 W low-pressure mercury lamp (365 nm)	172 organic compounds, alkanes, alkenes, arenes, non-substituted alkanols, substituted alkanols, alkenols, phenols, alkanals, alkenals, benzaldehydes, ketones, carboxylic acids, alkanoates, phthalates, nitrogen-containing organic compounds, sulfur-containing organic compounds and other species	140

photocatalytic depolymerization. These products suggested that native lignin could be converted into monomers by β-ether bond cleavage.

To fully utilize the entire lignocellulosic biomass, a lignin-first approach was reported by Wu *et al.*[139] In this approach native lignin in lignocellulosic biomass was converted into value added chemicals by cadmium sulfide quantum dots with MPA ligand (CdS QDs-MPA) while cellulose and hemicellulose remained almost fully intact. Furthermore, the colloidal character of quantum dots enabled their facile separation and recycling by a reversible aggregation–colloidization strategy. With birch woodmeal as substrate the major products were syringyl- and guaiacyl-derived ketones due to β-O-4 bond cleavage and the total yield of monomeric aromatics generated was 26.7 wt%. Lu *et al.*[140] described the photocatalytic depolymerization of rice husk over TiO_2 in an aqueous H_2O_2 (30%) solution with a 500 W mercury lamp. GC-MS confirmed the presence of 172 organic species in the product extract. Alkanes, phthalates and ketones were the largest groups of products.

In summary, research on photoconversion of lignocellulosic biomass has been conducted since the 1980s. The huge differences between raw biomass and model compounds have led to the fact that research is still trying to expand from model compounds to real-world biomass. From a feedstock perspective, real-world lignocellulosic biomass is derived from crops and wood, with a recalcitrant structure of cellulose, hemicellulose, and lignin crosslinked with each other meaning existing photocatalytic materials perform poorly. Moreover, the water-insoluble nature further reduces the efficiency of conventional photocatalytic suspension systems, and the use of organic solvents increases the cost and may generate pollution as well. To increase the hydrogen yields, most studies have reported the use alkali pre-treatment of biomass, thus further increasing the potential cost of the process. The substrate remaining after the photocatalytic hydrogen production reaction has also not been considered in detail and the remaining organic components may cause secondary pollution if discharged without additional treatments. Many high-value chemicals generated during photoreforming require subsequent separation and purification before utilization. From a material point of view, the most widely used material for hydrogen production is Pt/TiO_2, which is expensive due to the scarcity of precious metals and it is still challenging to recover and reuse the photocatalyst materials from the reaction system. Other low-cost photocatalytic materials have not yet reached the level of commercial production of titanium dioxide and are therefore still far from practical application.

Table 1 presents an overview of the valorisation of a range of "real-world" biomass materials which have been investigated using semiconductor photocatalysis.

2.2 Waste plastics

For the past century plastics have been an inherent part of our daily lives with the development and production of new plastic products really gaining momentum after WWII. Plastics are extremely versatile, and they have revolutionized almost every aspect of our lives, from medicine to cutting food waste and conserving energy.[141] They are cheap, convenient, light weight, durable and have an almost indestructible morphology. It is these highly desirable properties that make plastic the ideal material for such a wide range of applications that has resulted in the current environmental plague of plastic pollution. Single use plastics, such as plastic bottles can take up to 450 years to decompose and 500 years for a plastic toothbrush to decompose.[142] Globally only 9% of plastic waste is recycled, 19% is incinerated, 50% ends up in landfill and 22% evades waste management.[143] While landfill and incineration are low cost and simple disposal methods, they are extremely detrimental to the environment.[144] Since 1950, over 8 billion tons of plastic have been produced, over 80% of which has become either waste in landfills or in the natural environment[145,146] and it has been estimated that *ca.* 8 million tons of plastic enters the oceans every year. In 2016 alone, it has been estimated that up to 23 million tonnes of plastics entered aquatic ecosystems.[147,148]

In the Pacific Ocean there is a "garbage patch" of floating plastic denoted as the 7th continent.[149] At a size of 1.6 million square kilometres, it is more than 3 times the size of France and 2 times the size of Texas. The "garbage patch" is estimated to contain 80 thousand tons of plastic and 1.8 trillion pieces of plastic (microplastics constitute 94% of the patch) which has been exponentially increasing since the 1970's. As larger pieces of plastic making up the patch such as discarded fishing gear, bottle caps, crates and containers eventually break down they have the potential to increase the levels of microplastics by approximately 30-fold to around 50 trillion particles.[150] The great pacific garbage patch can be seen in Fig. 6.

Very recently microplastics (ranging from 5 to 10 μm in size) were detected in human placenta samples.[151] The microplastics were identified as pigmented polypropylenes which are used in paints, coatings, adhesives, plasters, polymers, dyes, cosmetics, and personal care products.[152] It is thought that microplastics access the bloodstream from either the maternal

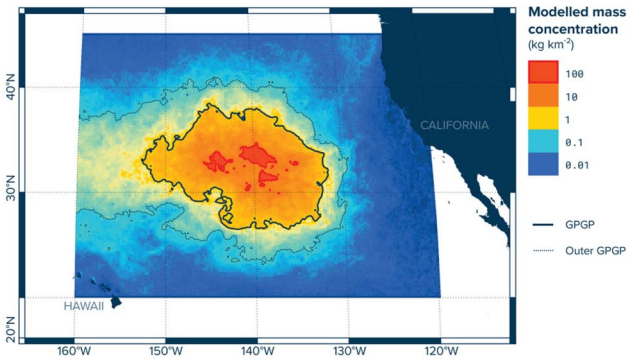

Fig. 6 The mass concentration model, pictured above, shows how the concentration levels gradually decrease by orders of magnitude towards the outside boundaries of the GPGP (great pacific garbage patch). The centre concentration levels contain the highest density, reaching 100 s of kg km^{-2} while decreasing down to 10 kg km^{-2} in the outermost region. Reproduced from ref. 150 with permission from the Ocean Cleanup.

gastrointestinal tract or respiratory system and then enter the placenta. Microplastics were found in both the maternal and foetal sides of the placenta as well as the chiromantic membranes. This may cause a range of detrimental effects on a developing foetus including triggering an immune response and the release of toxic contaminants that could lead to adverse pregnancy outcomes. With microplastics found in placenta, it is no surprise they have also been found in human blood,[153] faeces,[154,155] gastrointestinal tract,[156] lungs,[157] liver tissue, brain,[158] spleen and kidney tissues.[159,160] Humans are exposed to microplastics and by a variety of different methods, such as the consumption of contaminated marine animals,[161] drinking water (tap and bottled),[162] and foodstuff,[163–165] such as honey, salt sugar, beer, vegetables, fruits,[166] dairy,[167] meat,[168] soft drinks, tea,[169] and cereals, as well as in agricultural soil.[170] Additionally, exposure comes from use of cosmetics, toothpaste, and pharmaceuticals.[171–175]

Plastic waste is a persistent, abundant, cheap feedstock with both enormous challenges and potential. Plastic waste stores a significant amount of chemical energy which can be recovered to meet energy demand. The valorisation of plastic waste presents a significantly untapped opportunity to address environmental issues while also creating an economic push for a circular economy. While there has been significant research using pure control samples of *e.g.*, PVC and polystyrene, it is absolutely crucial to investigate real-world plastic samples, as they typically contain additional filters, cross-linkers or antioxidants that could make photoreforming more challenging. This section outlines the current literature on the photocatalytic reforming of plastic waste.

2.2.1 Photocatalytic degradation of waste plastic. As discussed in the previous section, plastic pollution is an increasing burden on the environment and there is an urgent need for new technologies to facilitate the removal of these materials. Photocatalytic degradation is an efficient and green technique currently used as a method to remove pollutants from water.[176] Pollutants such as pesticides, herbicides, insecticides,[177–180] pharmaceuticals,[181,182] dyes,[183,184] oils,[185] bacteria and their toxins,[186] and plasticizers[187] can be removed efficiently and economically by photocatalytic degradation technologies.[188–192] These technologies have been widely investigated and applied to the treatment of plastic waste into CO_2, water and microplastics for decades.[193–196] Obviously with current environmental concerns over CO_2 and net zero strategies, the production of CO_2 is highly undesirable and thus in this section we will focus on the photoreforming, rather than degradation, of plastic waste to produce value added materials and fuels in addition to tackling the plastic waste problem.

2.2.2 Photoreforming of waste plastic. Plastic waste has the potential to be a valuable feedstock with the ability to produce fuels and value-added chemicals from a persistent increasing pollutant.[197,198] Kawai and Sakata first described the photocatalytic production of hydrogen from PVC in 1981 using a 5% Pt/TiO_2 catalyst. After 10 h irradiation of a 500 W Xe lamp, 20 μmol, 17 μmol and 45 μmol of H_2 were produced using polyvinylchloride, polyethylene and polyvinyl alcohol respectively. When the photocatalysis was performed in a concentrated NaOH solution, hydrogen production increased to 45 μmol, 93 μmol and 86 μmol using polyvinyl chloride, polyethylene and polyvinyl alcohol, respectively. The authors attributed the enhanced H_2 production in alkaline solution to the formation of OH radicals from –OH which is formed when NaOH reacts with CO_2.[199]

More recently, Reisner *et al.*[200] investigated the photoreforming of 3 commonly produced polymers: polyethylene terephthalate (PET), polylactic acid and polyurethane over toxic yet inexpensive CdS/CdO_x quantum dots. The process operated under ambient conditions using visible light to produce pure H_2 and organic products such as formate, pyruvate, and acetate. Activity of the photoreforming system for PET and PU was found to be 12.4 and 3.22 mmol H_2 per g_{Cds} per h respectively. Following an alkaline hydrolysis, monomers were released into solution which could be reused. Real-world applicability has been demonstrated by photoreforming a PET water bottle to produce H_2 using CdS/CdO_x. Over the course of 6 days of photocatalytic reaction, there was continuous generation of H_2, with 4.13 mmol H_2 per g CdSs per h generated, with an external quantum yield of 2.17% and a conversion efficiency of 5.15% (Fig. 7).

The Reisner group has also investigated the photoreforming of plastic using a non-toxic and non-precious metal containing carbon nitride with nickel phosphide cocatalyst CN_x/Ni_2P.[201] Initial tests were carried out to convert PET and PLA to H_2 and chemicals including acetate, formate and glyoxal as well as hydrogen. Following the successful conversion of PET and PLA, real-world substrates including polyester fibres and an oil contaminated PET and a non-contaminated PET water bottle

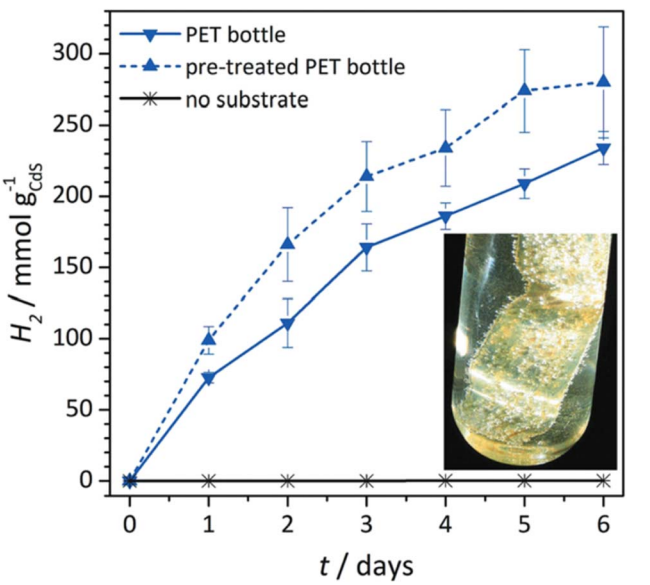

Fig. 7 Long-term photoreforming of a PET bottle to H_2 using CdS/CdO_x QDs (1 nmol) under simulated sunlight (6 days, AM 1.5 G, 100 mW cm^{-2}, 25 °C). Conditions: ground PET bottle (25 mg ml^{-1}) freshly prepared or pre-treated in 10 M aq. NaOH (2 ml). Inset: photograph of a PET bottle sample; H_2 bubbles are visible on the plastic surface. Reproduced from ref. 200 with permission from the Royal Society of Chemistry.

were also successfully photoreformed. After 5 days of irradiation in the presence of the photocatalyst, the hydrogen yields of 104, 22 and 11.4 μmol H_2 per g sub. were obtained for polyester fibres, PET bottle and the oil contaminated PET bottle respectively. As the reaction progressed, the surface area of the fibres exposed during the reaction increased, which resulted in an increasing rate of reaction over time. The oil contaminated PET bottle had a low yield due to the oil preventing access to the PET water bottle by the reactive oxygen species. Additional fillers and lower solubility of the real-world substrates were thought to result in the poorer performance of these materials compared to pure samples. The photocatalytic process was scaled up successfully from 2 ml to a 120 ml system.

The Reisner group[202] have recently shown a visible light-driven reaction to deconstruct real-world polystyrene into benzoic acid and other monomeric aromatic products at 50 °C under ambient pressure. A range of fluorenone photocatalysts (*e.g.* 9-fluorenone, 2-bromo-9-fluorenone and 2, 7-dicholoro-9-fluorenone) were tested and irradiated under blue LED light with 1 equivalent of H_2SO_4 and oxygen supplied in a balloon. It was determined that a fluorenone loading of 20 mol% was required for the optimum benzoic acid yield (38% after 48 h over 9-fluorenone). The reaction was then scaled up to the gram scale to investigate the deconstruction of pure polystyrene and real-world polystyrene foam. In the case of pure polystyrene, after 64 h photocatalysis the yield of all aromatic compounds was 60 ± 2% (including 36 ± 4% benzoic acid). Conversion of the real-world polystyrene foam produced a similar product distribution with 60 ± 4% aromatic compound yield and 36 ± 2% yield of benzoic acid after 72 h of photocatalysis. The reaction was believed to proceed *via* a C–H bond oxidation pathway over all catalysts and allowed valuable products to be generated from real-world waste plastic.

Li *et al.*[203] prepared a series of $MoS_2/Cd_xZn_{1-x}S$ photocatalysts for solar H_2 production coupled with the degradation of plastics. 4.3 wt% MoS_2 integrated $Cd_{0.5}Zn_{0.5}S$ exhibited the highest H_2 evolution rate of 15.90 mmol h^{-1} g^{-1} and H_2 yield of 80 mmol g^{-1} from a PET based aqueous alkaline solution. This enhanced H_2 production over this material was attributed to the synergetic effects in terms of charge separation efficiency, light absorption capability and suitable oxidation potential. Various loadings of MoS_2 were investigated. The presence of any loading of MoS_2 compared to no loading was found to enhance the H_2 evolution compared to no loading, which was attributed to the MoS_2 material providing more active sites to facilitate proton reduction and accelerate photoexcited carrier separation. A loading above 4.3 wt% MoS_2 was found to be detrimental to photocatalytic activity. 4.3 w% MoS_2 was determined to be the optimum loading resulting in the best H_2 yield and production rate. This study was further extended to a PET plastic bottle,

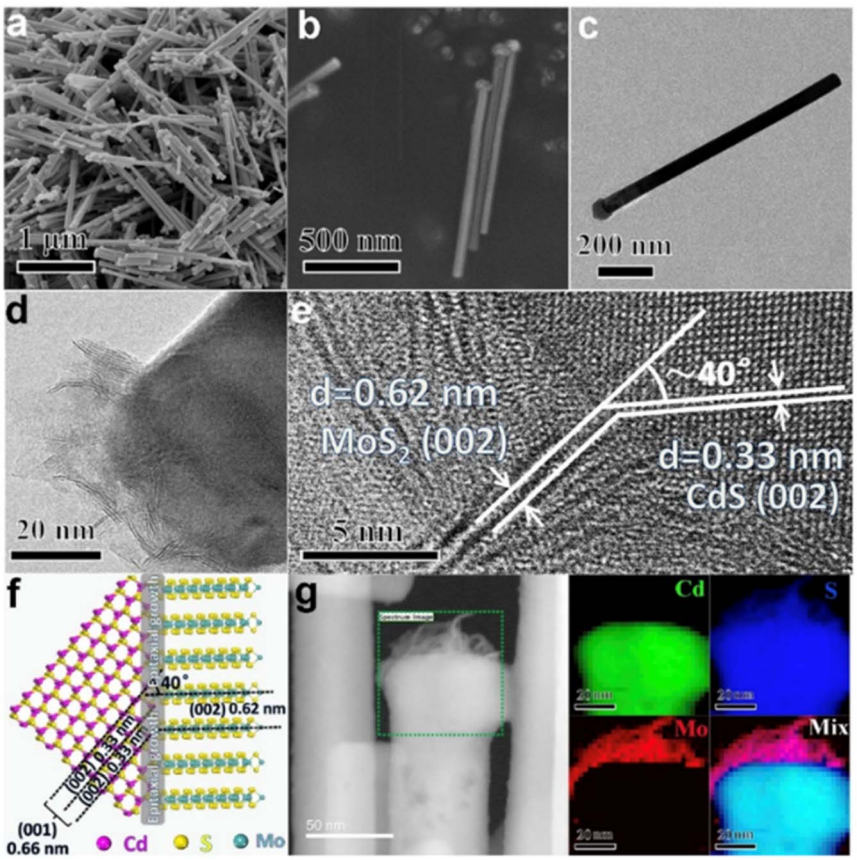

Fig. 8 (a and b) SEM and (c and d) TEM images of the MoS_2/CdS and (e) MoS_2/CdS interface convinced by HRTEM and (f) corresponding theoretical model; (g) element mapping of MoS_2/CdS. Reproduced from ref. 203 with permission from Wiley.

with a H_2 evolution rate of 14.9 mmol h^{-1} g^{-1} and an H_2 yield of 70 mmol g^{-1}. The eventual products of the PET bottle's photocatalytic reforming were formate, methanol, acetate and ethanol. PET/pieces of PET bottle were stirred in 10 M NaOH for 24 h at 40 °C, then the mixture was centrifuged, and the supernatant was used as the photocatalytic substrate. SEM and TEM images of the catalysts used in this study can be found in Fig. 8.

Du *et al.*[204] described the synthesis of MoS_2 tipped CdS nanorods for the photocatalytic reforming of plastic waste into commodity chemicals and hydrogen. The CdS nanorod behaved as the light absorber and a hole acceptor while MoS_2 acted as an electron collector (Fig. 8). The spatial separation of these two components enabled fast charge migration to achieve a long-lived charge carrier. Like other studies the plastics were subjected to a pre-treatment step with 10 M KOH or HNO_3 depending on the plastic. Using PLA as the substrate it was found that a higher rate of H_2 was produced (3–6.2 mmol g^{-1} h^{-1}) as the concentration of KOH was increased from 1–10 ml over a 21.8 wt% MoS_2/CdS catalyst respectively. This enhanced activity was attributed to the higher concentration of lactate in solution as the alkalinity of the solution was increased. As the MoS_2 loading was increased the H_2 formation increased up to a loading of 21.8 wt%. A further increase in the loading of MoS_2 to 46.2 wt% resulted in a decrease in H_2 formation. After photocatalysis over a 21.8 wt% MoS_2/CdS catalyst for 25 h, the total H_2 evolved was 95 mmol g^{-1} from pre-treated PET. Encouragingly the total H_2 evolved from a pre-treated PET bottle was 85 mmol g^{-1} after 25 h. Using pre-treated PLA as the substrate resulted in *ca* 160 mmol per g H_2 produced after 25 h of photocatalysis.

Xie *et al.*[205] developed a universal photoinduced C–C cleavage and coupling pathway for converting waste plastics into high-energy-density C2 fuels under atmospheric conditions. Using the developed pathway Xie and co-workers were able to selectively photoconvert real-world plastics such as plastic bags, disposable food containers, food wrap films and their main components of polyethylene, polypropylene and polyvinylchloride into C2 fuels using single-unit-cell thick NbO_2 layers and sunlight. In the case of polyethylene, polypropylene and polyvinylchloride, 100% of these materials were photocatalytically degraded to CO_2 gas within 40, 60 and 90 h, respectively. The CO_2 was then photoreduced to acetic acid *via* the same catalyst with formation rates of *ca.* 47.4, 40.6 and 39.5 μmol g_{cat}^{-1} h^{-1} respectively being reported.

A novel floating carbon nitride composite was developed for the solar reforming of waste plastics and biomass in a very recent study by Reisner *et al.*[206] CN_x/Pt and CN/NiP were immobilised on hollow glass microspheres (HGM) which acted as supports enabling the catalytic material to float and overcome limitations such as turbid waste streams (Fig. 9) Not surprisingly, solar reforming activity was highest over Pt (0.91%) deposited on CN with a specific activity of 78.2 ± 7.5 μmol_{H_2} g_{CNx}^{-1} h^{-1} for KOH pretreated PET. The specific activity was found to increase to 99.9 ± 2.6 μmol_{H_2} g_{CNx}^{-1} h^{-1} using the same catalyst following reaction scale up and recycling.

Photoreforming of plastic waste has huge potential to combat plastic pollution as well as generating value added chemicals and hydrogen, thus contributing to a circular economy and helping towards achieving net zero targets. However, adding value to plastic is not without its challenges. Currently the plastics undergo some sort of undesirable pre-

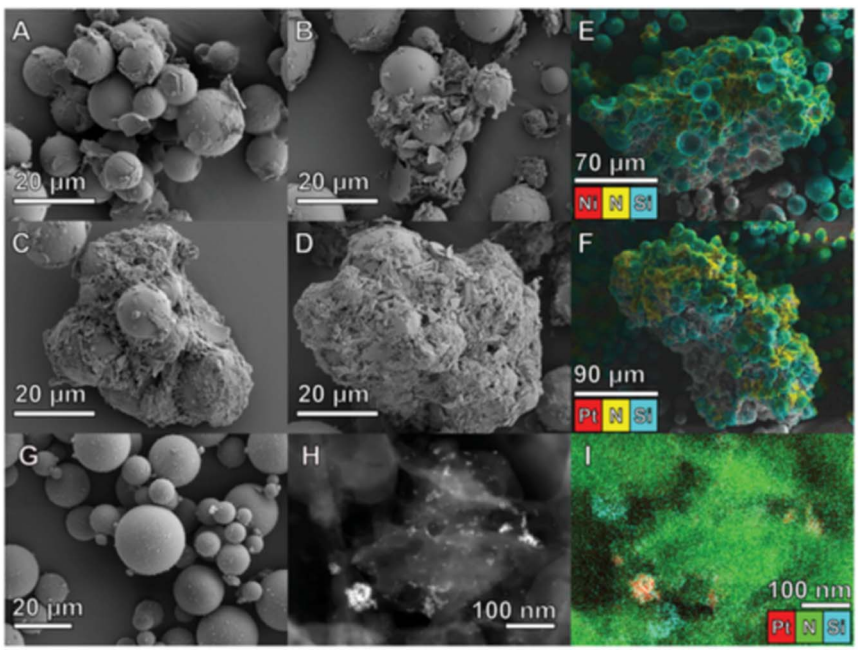

Fig. 9 SEM images showing the morphology of floating CN_x composites differentiated by their HGM : melamine ratio. (A) 1 : 1, (B) 1 : 2, (C) 1 : 3, (D) 1 : 4 (scale bar shared by panels A–D), (E) coloured EDX overlay showing Ni, N, and Si of 1 : 3 with a Ni_2P co-catalyst, (F) coloured EDX overlay showing Pt, N and Si of 1 : 3 with a Pt co-catalyst, (G) Im30K glass bubbles, (H) STEM-HAADF of HGM/CN_x|Pt (1 : 3) showing elemental contrast, (I) EDX overlay on STEM-HAADF of HGM/CN_x|Pt (1 : 3) showing Pt, N and Si. Reproduced from ref. 206 with permission from Wiley.

Table 2 Summary of real-world plastic substrates for photocatalytic valorization

Feedstock details	Catalyst	Experimental conditions	Product details	Reference
PVC PE PVA	5% Pt/TiO_2	500 W Xe lamp Alkaline hydrolysis pretreatment	PVC: 45 μmol H_2 PE: 93 μmol H_2 PVA: 86 μmol H_2	199
PET PLA PU PET water bottle	CdS/CdO_x	Ambient conditions and visible light Alkaline hydrolysis pretreatment	PET: 12.4 mmol H_2 per g_{Cds} per h PU: 3.22 mmol H_2 per g_{Cds} per h PET water bottle: 4.13 mmol H_2 per g_{Cds} per h external quantum yield; 2.17% conversion; 5.15%	200
PET PLA Polyester fibres PET water bottle oil contaminated PET water bottle	CN/Ni_2P	Alkaline hydrolysis pretreatment Visible light	PET: acetate 190 nmol, formate 190 nmol, glyoxal, 9300 nmol PLA: acetate 100 nmol, formate 95 nmol Fibres: 104 H_2 per g sub. PET water bottle: 22 H_2 per g sub. Contaminated PET water bottle: 11.4 μmol H_2 per g sub.	201
PS pure PS foam	20 mol% fluorenone	50 °C Blue LED 1 eq. of H_2SO_4 O_2 balloon	Pure PS: 60% aromatic compounds PS foam: 60% aromatic compounds	202
PET PET water bottle	$MoS_2/Cd_xZn_{1-x}S$	Alkaline hydrolysis pretreatment	PET: 80 mmol per g H_2 PET water bottle: 70 mmol per g H_2 plus additional products such as formate, methanol, acetate, ethanol	203
PLA PET PET water bottle	21.8% MoS_2 tipped CdS nanorods	Alkaline/acid hydrolysis pretreatment 300 W Xe lamp illumination equipped with an AM 1.5 solar simulator	PLA: 160 mmol per g H_2 PET: 95 mmol per g H_2 PET water bottle: 85 mmol per g H_2	204
Pure PE Pure PP Pure PVC Food container Food wrap film Single use bag	Nb_2O_5	300 W Xe lamp illumination equipped with an AM 1.5 solar simulator O_2 atmosphere	Evolution rate of acetic acid Pure PE: 42.6 μg g_{cat}^{-1} h^{-1} Pure PP: 39.6 μg g_{cat}^{-1} h^{-1} Pure PVC: 37.8 μg g_{cat}^{-1} h^{-1} Food container: 20.8 μg g_{cat}^{-1} h^{-1} Food wrap film: 19 μg g_{cat}^{-1} h^{-1} Single use bag: 24.6 μg g_{cat}^{-1} h^{-1}	205
PET	Floating CN_x, CN_x|Pt, CN_x|Ni_2P	Vertical simulated solar irradiation (AM 1.5 G) Alkaline hydrolysis pretreatment	PET: 78.2 ± 7.5 $umol_{H_2}$ per g_{CNx} per h H_2	206

treatment such as alkaline hydrolysis and the use of real-world contaminated plastic remains a further challenge. Table 2 provides an overview of some of the key research undertaken to date on photocatalytic reforming of plastic materials.

2.3 Wastewater

Industrial wastewater or effluents is one of the most frequently exposed waste resources in our daily life.[207] Industrial wastewater can be resource-rich in nutrients and chemical compounds.[208] It can contain a broad range of contaminants including heavy metals, organic matter, inorganic particles, toxins, pharmaceuticals, agrichemicals, and microplastics. Chemical oxygen demand (COD) is a measure of the capacity of water to consume oxygen during the decomposition of organic matter in the water.[209] For example, an average COD of 11 000 mg L^{-1} is generated from paper and pulp industries every year,[210] and the value is 16 000–100 000 mg L^{-1} for palm oil mill effluent.[211] The organic matter in industrial wastewater is potentially the most valuable part which could be reformed through various technologies generating value-added products and energy, especially through a sustainable process such as photocatalysis.[212–214] Based on the basics of photocatalytic process in the system of water, the generated reactive species, *i.e.*, hydroxyl radicals ($^{\bullet}OH$) and superoxide radicals ($^{\bullet}O_2^-$), can provide the redox potential of the reactions of organic matter adsorbed on the photocatalysts,[215] which leads to the reforming/degradation of organic matter and production of H_2 energy. The following considers the current state-of-the-art research on the photocatalytic process of a real-world feedstock: industrial wastewater effluents.

Effluents from the food industry (*i.e.*, juice,[216,217] olive oil[218,219]) were studied mostly as a feedstock for photocatalytic H_2 production. H_2 yields of 115 μmol $g_{catalyst}^{-1}$ h^{-1} were reported using an Au/TiO_2 material for the photocatalytic reforming of wastewater from juice manufacture. This was significantly higher than yields of hydrogen from the photoreforming of municipal wastewater in the same reactor. The relatively higher production rate of H_2 was potentially due to the significant level of saccharides contained in the wastewater from the juice manufacturing process.[216] It was reported, however, the wastewater from fruit bottling plants with higher initial DOC content (600 mg L^{-1} in fruit bottling wastewater vs. 100 mg L^{-1} in municipal wastewater) resulted in lower H_2 production compared to that produced from municipal wastewater following THE photocatalysis of the effluent.

Therefore, the concentration of organic matter in the effluents is not the only consideration affecting the reactivity of H_2 production from industrial wastewater. Badawy *et al.*[218] investigated the effect of the pH of olive oil industrial wastewater on its photoreforming reactivity over a mesoporous TiO_2 photocatalyst. According to their study, an acidic pH was favourable for the photocatalytic degradation of organic compounds due to the improved adsorption of organic compounds onto the TiO_2 surface and therefore facilitated the photocatalytic degradation process. An acidic pH value was also reported to benefit the H_2 production from the photocatalytic reforming of olive oil industrial wastewater. This positive influence was believed to be from:

(i) the positions of the valence-band and conduction-band levels of the semiconductor with respect to those of redox couples in solution,

(ii) the charging behaviour of the TiO_2 surface, and

(iii) the competitive adsorption of organic pollutants on the TiO_2 surface.

Moreover, it was reported by Speltini *et al.*[219] that the H_2 yield could be significantly enhanced (an increase of the yields to 81%) by performing a simple clean-up (magnesium silicate as a clean-up sorbent) of the raw olive oil wastewater which resulted in the removal of species which could potentially foul the photocatalyst surface, for example lipidic compounds. Partial deactivation of Pt/TiO_2 for H_2 production was observed from the presence of oil and grease compounds, and inorganics (F^-, Cl^-, PO_4^{3-} and SO_4^{2-}) in the olive oil wastewater effluent.[219]

The photocatalytic degradation of the organic matter present in effluents from the paper and cellulose industry was reported by Machado *et al.*[220] The pH, the use of additives, and the morphology of the photocatalyst were reported to influence the degradation efficiency considerably. Acidic pH (<4) was beneficial to the degradation efficiency observed for effluents containing lignin and cellulose pulp. The use of a P25 TiO_2 photocatalyst resulted in a 60% higher degradation rate than that obtained when an anatase TiO_2 material was used for the photocatalytic degradation of that effluent. The addition of hydrogen peroxide in the reaction system over P25 TiO_2 increased the efficiency of the photocatalytic process by over 170%.

Other effluents such as municipal wastewater were also investigated as real-world feedstocks for photocatalytic H_2 production.[216,217] H_2 production was limited over $^{H,DP}Cu/TiO_2$ and $^{H,DP}Au/TiO_2$ photocatalysts as reported by Imizcoz *et al.*[216] The efficiency of H_2 production (21 μmol H_2 per L wastewater) and organic pollutant removal (15% of dissolved organic carbon, DOC) *via* photocatalysis over Au/TiO_2 in municipal wastewater at pilot-plant scale (5 h irradiation under direct solar light in a Compound Parabolic Collector reactor, CPC reactor, accumulated radiation energy of 110 kJ L^{-1}) was reported by Salgado *et al.*[217] Based on their studies, the chemical nature and the concentration of organic compounds present in the real wastewater effluents significantly influenced the photocatalytic reactivity. Furthermore, the presence of high concentrations of Cl^- and SO_4^{2-} ions was found to reduce the photocatalytic activity for H_2 generation.[217]

Secondary effluent from a municipal wastewater treatment plant was also investigated as feedstock for H_2 production over $P–TiO_2/Pt$ microspheres.[221] In this study, the dissolved organic matter and inorganic ions in secondary effluent were isolated into four fractions, *i.e.*, hydrophobic acids (HOA), hydrophobic bases (HOB), hydrophobic neutrals (HON), and hydrophilic substances (HIS). Among those species, the decomposition of humic/fulvic acid-like substances in the HIS fraction played a role in accelerating hydrogen production and removal of estrogenic substances. This was proposed to be a result of the electron donors (*i.e.*, formaldehyde, acetaldehyde, acetate, and

Table 3 Summary of real-world wastewater substrates for photocatalytic valorization

Feedstock details	Catalyst	Experimental conditions	Product details	Reference
Juice production wastewater Municipal wastewater	$^{H,DP}Au/TiO_2$ and $^{H,DP}Cu/TiO_2$ 25 mg	Simulated solar light (AM 1.5 G, 1.0 kW m^{-2}) 25 °C Ar atmosphere No pre-treatment	Juice production wastewater $^{H,DP}Au/TiO_2$: <0.1 μmol per g_{cat} per h H_2, 15.8 μmol per g_{cat} per h CO_2 $^{H,DP}Cu/TiO_2$: 0.1 μmol per g_{cat} per h H_2, 18.2 μmol per g_{cat} per h CO_2 Municipal wastewater $^{H,DP}Au/TiO_2$: 115.1 μmol per g_{cat} per h H_2, 306.9 μmol per g_{cat} per h CO_2 $^{H,DP}Cu/TiO_2$: 10.7 μmol per g_{cat} per h H_2, 291.2 μmol per g_{cat} per h CO_2	216
Juice production wastewater Municipal wastewater	0.5 wt% Au/TiO_2	Irradiation of natural sunlight for 5 h, pH = 3	Methanol: 0.5 × 10^3 μmol per L H_2 Glycerol: 4.5 × 10^3 μmol per L H_2 Formic acid: 6.5 × 10^3 μmol per L H_2 Juice production wastewater: 5.2 μmol per L H_2 Municipal wastewater: 17.5 μmol per L H_2	217
Olive mill wastewater	Mesoporous TiO_2	UV mercury lamp (150 W, 1.32 × 10^{-5} einstein per s), pH = 5.4	Olive mill wastewater: initial H_2 production rate (first 120 min): 0.18 mmol per min H_2 Olive mill wastewater: H_2 production rate (after 240 min): 0.104 mmol per min H_2	218
Olive mill wastewater	0.3 wt% Pt/TiO_2 Eosin Y/Pt/TiO_2	Irradiation of a UV-A lamp (flux 5.8 × 10^{-7} mol photons per s) pH = 3 Pre-treatment with magnesium silicate (125 g L^{-1}, 6 h) Under irradiation of a solar light simulator (250 W m^{-2})	Under UV-A irradiation for 4 h Olive mill wastewater: 44 μmol and 80 μmol (pre-treated) of H_2 Consecutive irradiation cycles 4 × 4 h under UV-A Olive mill wastewater: 280 μmol of H_2 Glucose: 343 μmol of H_2 Under irradiation of solar light simulator Olive mill wastewater: 66% H_2 with respect to that obtained by UV-A irradiation	219
Effluent from a paper and cellulose mill	TiO_2	400 W mercury lamp (1100 W m^{-2}), pH = 3 Pre-degradation treatment of lignosulphonate	COD reduction/removal in 180 min: lignosulphonate: 15% Pre-degraded lignosulphonate: 62% Effluent: 78%	220
Secondary effluent from a municipal wastewater treatment plant	P–TiO_2/Pt microspheres	450 W solar-light simulator (400–750 nm, 4.6 × 10^{-7} einstein per s) 5 h irradiation	H_2 production from each group of compounds in the effluent De-aerated system: 0.2 μmol of H_2 (HIS), 6.8 μmol of H_2 (HOA), 1.2 μmol of H_2 (HOB), 2.2 μmol of H_2 (HON) Dissolved oxygen-decreasing system 9.3 μmol of H_2 (HIS), 1.7 μmol of H_2 (HOA), 0.3 μmol of H_2 (HOB), 1.6 μmol of H_2 (HON) Hydrophobic neutrals (HON), hydrophobic bases (HOB), hydrophobic acids (HOA), hydrophilic substances (HIS)	221

formate) being generated from the decomposition of humic/fulvic acid-like substances by reactive oxygen species (ROS, *i.e.*, h^+, $^{\bullet}OH$, and $^{\bullet}O_2^-$) in the aerobic reaction system, which could significantly improve the efficiency of H_2 production.

Based on the reports for photocatalytic reforming/degradation of real-world effluents, the concentration of organic matter in the effluents and the pH value of the effluents could significantly influence the efficiency of photocatalytic reforming/degradation processes. The chemical composition of the effluents was also important, for example, the lipidic compounds, oil and grease, as well as the inorganics such as F^-, Cl^-, PO_4^{3-} and SO_4^{2-} could potentially deactivate the photocatalysts in the reaction systems. Therefore, pre-treatments such as precipitation and filtration, and pH adjustment of the effluents were required to obtain an efficient photocatalytic treatment process. TiO_2-based noble metal photocatalysts have been frequently investigated for their ability for use in photocatalytic reforming/degradation of wastewater effluents. To further improve the efficiency of the photocatalytic reforming/degradation of real-world effluents, cheaper and highly efficient photocatalysts will need to be developed. The inorganic and metal content present in the industrial wastewater could also be considered as sources of materials for the preparation of photocatalysts.

Table 3 provides an overview of a range of industrial wastewater effluents that have been used for photocatalytic reforming processes.

3. Comparison of different reforming methods for H_2 production

Among all the reforming methods for H_2 production (Table 4), steam reforming showed a relatively high technology readiness level (TRL), for example, a value of 9 for steam methane reforming (SMR) which has been commercialised. In the process of SMR, H_2 was produced with CO and a small amount of CO_2 through the reaction of methane and steam. Partial oxidation (POX) of the feed by limited oxygen can release heat during the oxidation, which is normally integrated with SMR. This process is called autothermal reforming (ATR). Apart from methane, propane, gasoline, coal and natural gas can also be used as feed in the ATR process for H_2 production with a high efficiency of 60–75%.[223]

H_2 generation from aqueous phase reforming (APR) and dry reforming (DR) has medium TRL levels. In the process of APR, hydrocarbons can react with water at mild temperature between 220 and 270 °C and high pressure (30–60 bar).[224] The efficiency of H_2 production from APR can reach more than 55% with the challenges of activating catalysts in short time that requires a large-scale reactor.[225] Alcohols (methanol, ethanol), polyalcohol (ethylene glycol, glycerol, xylitol, sorbitol), and complex matrixes such as glucose, xylose, and woody biomass can all be used as the feed in the procedure of APR for H_2 generation. DR is the process during which CO_2 reacts with methane to form syngas. The highest energy efficiency of 70% can be reached at 1000 K accompanied by a conversion of 83%.[226] Coking and sintering of the catalyst at high temperature are the two major problems related to a loss in activity of DR.

Other reforming technologies for H_2 generation such as electro-reforming (ER) and plasma-assisted reforming (PR) have relatively low TRL values, which require a long term (>10 years) to achieve commercial maturity.[227] The process of ER can be seen as a reaction of proton reduction in acidic media and water reduction in alkaline media at the cathode with the oxidation of oxygenated organic compounds (OOCs) at the anode of an electrolysis cell. It is less mature than H_2 production from other electro-technologies such as water electrolysis (*e.g.*, TRL 9 for alkaline electrolysis and TRL 5–7 for proton exchange membrane electrolysis).[228] However, the ER process has important advantages such as clean H_2 production without downstream purification processes and the possibility of coproduction of value-added compounds at the anode of the electrolysis cell. PR for H_2 production is developed from the conventional reforming method and it showed many benefits such as broad range of feed/fuels, fast response, and high conversion efficiency of up to 85%.[229] In the procedure of PR, diesel, biomass, gasoline, oil, jet fuel, and natural gas can be used as feed.

H_2 generation from photocatalytic reforming as an "emerging" technology has a low TRL (<4) compared to conventional technologies such as SMR (or ATR, TRL = 9) and DR (TRL = 5). Compared to other "emerging" technologies such as ER and PR, photoreforming technology also showed a broad acceptance of feeds, including from simple molecules to complex matrixes. Additionally, the requirement of energy input from solar or electricity (*i.e.*, artificial light) makes it more sustainable and flexible in terms of energy consumption. It is

Table 4 Comparison of different reforming methods for H_2 production

Reforming technology	Input energy source	Feed/fuels	TRL
Steam reforming (auto thermal reforming)	Heat	Methane, propane, gasoline, coal, natural gas	High
Aqueous phase reforming	Heat	Alcohols, polyalcohol, oxygenated organic compounds (OOCs) from biomass	Medium
Dry reforming	Heat	Carbon dioxide, methane	Medium
Plasma-assisted reforming	Electricity	Hydrocarbons, diesel, biomass, gasoline, oil, jet fuel, natural gas	Low
Electro-reforming	Electricity	Methanol, formic acid, OOCs from biomass[222]	Low
Photo-reforming	Solar/electricity	OOCs from biomass, plastics, waste streams	Low

promising to generate H_2 with formation of value-added chemicals under mild conditions, although the photo-reforming technology still has a very low efficiency of conversion and energy use compared to other reforming technologies.

4. Perspective: the role of photocatalysis within a circular economy

Photocatalysis is frequently described as an "emerging" technology and one which is capable of being deployed across multiple applications. These applications are often considered under two broad areas of environmental remediation and energy production. The former is more advanced in relation to a Technology Readiness Level (TRL), while the latter is predicted to achieve substantial impact despite its current lower TRL status. Regardless of the TRL status or predicted impact, however, there are a limited number of examples demonstrating activity or efficiency at increased or industry level capacity. In more recent years, this point has been highlighted for both photocatalytic environmental remediation[230] and energy production.[218]

Transitioning photocatalysis towards pilot scale and even industry level deployment is challenging and dependent on several parameters. If the TRL scale is used as a metric for evaluating the technology, this complexity is clearly highlighted. For example, progression from a TRL of 4 to 5 represents a photocatalytic unit operating in a 'relevant environment', rather than a lab environment, which crucially is underpinned by industrial stakeholder engagement. Given that most of the photocatalytic research is typically focused on materials synthesis and improving fundamental understanding, achieving that transition will not be achieved quickly. Previous papers have also warned that if this trend continues, the technology transfer challenges are neglected which can be determinantal to the research field. Specifically, Loeb *et al.* stated that such a trend "ignores the immense technology transfer problems, perpetuating a widening gap between academic advocation and industrial application".[231] The technology transfer challenges are those that are represented by advancing the TRL of photocatalytic technology, specifically into the region of 4–6. Despite the challenges, however, it is possible to view evidence across multiple platforms which suggests the photocatalytic transition is beginning:

- The role of the literature: an increase in the number of perspectives, roadmaps and articles which focus on holistic system analysis represents an awareness of both the challenges and opportunities with advancing photocatalytic technology.
- Net zero emission targets and national strategies: legal binding targets have been set which have changed the global energy landscape and accelerated the need for renewable energy vectors such as hydrogen.

The first point refers to the publication of articles which are beyond research advancements and address a holistic view of photocatalysis. The paper by Loeb *et al.*[231] is an excellent example of this as it adopts a critical perspective of photocatalysis to highlight the key issues associated with the technology horizon. Furthermore, it also presents a way forward for the technology by suggesting key targets to be achieved. Our own previous article considered a similar approach but in relation to photocatalytic biomass reforming by coupling a review with a critical evaluation of the technology. The work by Skillen *et al.* concluded with a proposed roadmap and strategy for achieving technology deployment, which included four key points ranging from catalyst development that facilitates technology growth and not academic hype through to even distribution of research priorities[232] In relation to the latter point, there is evidence of this occurring with specific examples including the work by Rumayor *et al.*,[233] Bahnemann *et al.*,[234] and Nishiyama *et al.*[235] A recent lifecycle assessment (LCA) based study not only emphasized the potential for photocatalytic hydrogen production but highlighted the need for additional research in key areas. Rumayor and colleagues[233] demonstrated that photocatalytic waste (glycerol) reforming was within the portfolio of sustainable hydrogen production technologies based on kg CO_2 eq. In January 2023, a roadmap article was published by Bahnemann *et al.* for the *Journal of Physics: Energy*, which was a collection of articles that explored photocatalytic and photoelectrocatalytic hydrogen formation.[236] The collection considered low-carbon hydrogen generation from the perspectives of basic processes, materials science through to reactor engineering and applications for biomass reforming. The roadmap article was developed with a view towards the role that alternative or low-carbon technologies can play within the transition to net zero carbon economies. This key point was also reflected in the work by Welfle *et al.*, in 2023,[87] who considered photocatalysis alongside other conversion technologies when mapping the risk and benefits of future bioenergy systems. The research applied a Bioeconomy Sustainability Indicator Model (BSIM) to "map and analyse the performance of bioenergy across 126 sustainability issues". In order to achieve this, the authors considered 16 bioenergy case study scenarios which included:

- Hydrogen from biomass wastewater *via* photocatalysis.
- Hydrogen from miscanthus *via* photocatalysis.

In both case study scenarios, there was an assumed increase in the TRL status of photocatalysis to better evaluate the sustainability risks and benefits. The result of the modelling work (Fig. 10 and Table 5) highlighted that photocatalytic technology contributed towards several sustainability indicators, specifically highlighting 'innovation', 'replaced fuels' and 'water use and efficiency' as benefits. In contrast, 'techno-economics' was determined to be a sustainability risk in both scenarios. Given that an assumed increase in TRL status was applied for this study, it is expected that techno-economics would be a risk due to limited data to validate the feasibility of large-scale deployment. An interesting point worth noting, however, was that both case studies utilized a sustainable (miscanthus) or waste (wastewater) feedstock for hydrogen generation. This point is key as such an approach not only contributes towards net zero emission targets, but it also supports the role that photocatalysis can play in relation to enhancing and maximizing sustainable resource use. As

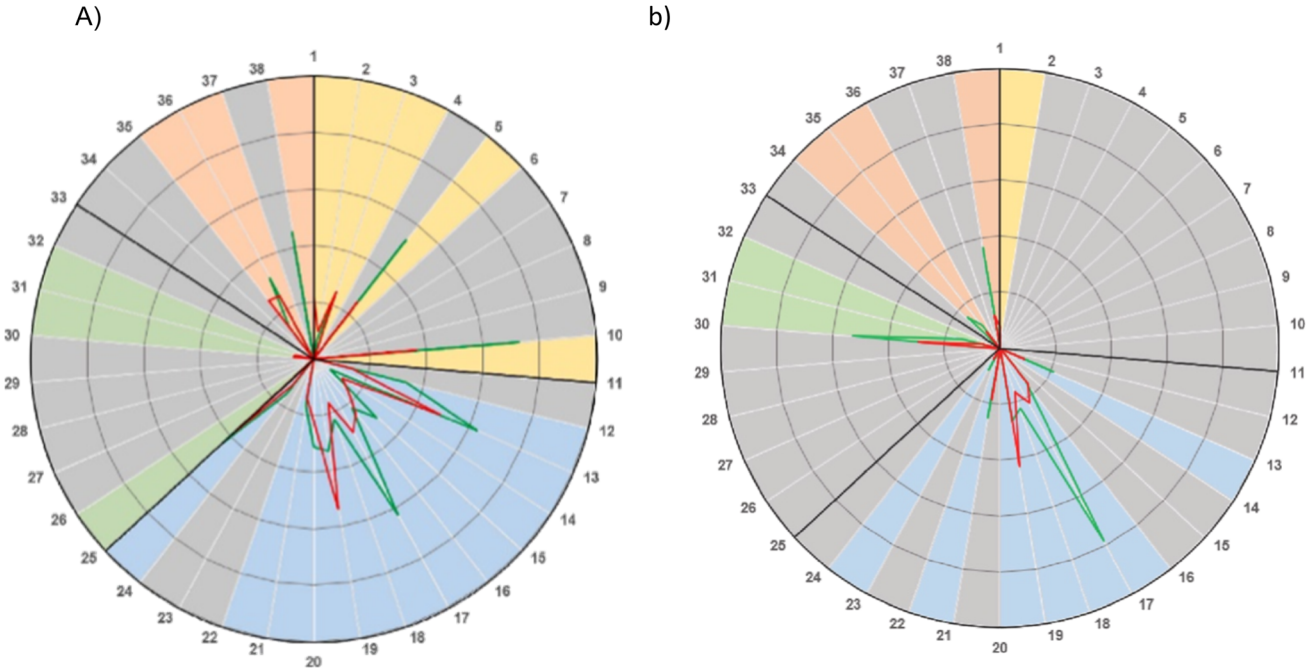

Fig. 10 BSIM results for photocatalytic hydrogen production within a bioenergy system highlighting sustainability risks and opportunities based on (a) photocatalytic hydrogen from biomass wastewater and (b) photocatalytic hydrogen from miscanthus reforming. Figure reproduced from ref. 87 with permission from Elsevier.

a result, it demonstrates that photocatalysis, as an emerging technology, can be a viable option within a circular economy.

The second driver behind a photocatalytic transition is countries establishing net zero emission targets coupled with appropriate legislation to support them. This has subsequently led to the development of national hydrogen strategies for the first time, which set out capacity targets for low-carbon hydrogen production. Both points are crucial as they have substantially and irreversibly altered the global energy landscape by accelerating the need for renewable energy systems to be deployed. As a result, there is increasing focus on current and emerging low-carbon technologies with the capabilities of producing renewable or 'green' fuels such as hydrogen. While electrolysis is expected to be the primary contributor towards renewable hydrogen targets as we approach 2030, it is becoming apparent that additional technologies will be needed. Net zero by 2050 is estimated to require approx. 4–5 TW of renewable hydrogen capacity; however, global production is currently only 0.7 GW. In order to reach such an ambitious target, a diverse collection of technologies will be required that are capable of being deployed across a broad range of sectors and geographies. The ability of these technologies to integrate into a circular economy will be a crucial consideration as reaching net zero is dependent on more than increased renewable energy production. There will be a substantial need to implement improved sustainable practices which include technology development. The emergence of biohydrogen and artificial photosynthesis (including photocatalysis) will be fundamental to that process.

At present there is of course a substantial gap between the current technology readiness status of photocatalysis and the status needed to contribute towards net zero. A specific challenge is the cost at which photocatalytic hydrogen could be produced. While the target for renewable hydrogen is \$1.5 per kg H_2, to date an accurate costing for photocatalytic hydrogen is yet to be established. A relative comparison, however, would be to biohydrogen production methods. A recent study by Ganeshan *et al.*[237] conducted a techno-economic analysis (TEA) and lifecycle assessment (LCA) of biohydrogen supply chains to determine production costs and their carbon footprint. The TEA determined a range of \$1.2–14.9 per kg H_2 based on biomass or wastewater feedstocks, while the LCA showed −1.6–12.2 kg CO_2 eq. per kg H_2 based on holistic systems analysis. The lowest production costs, which would be competitive with fossil-fuel derived hydrogen, were achieved for anaerobic digestion (AD) and biomass gasification at \$1.2 per kg H_2 and \$1.25 per kg H_2 respectively. Given that both technologies are already mature (TRL 9) and well established, a low production cost is to be expected. It is, however, worth nothing that microbial electrolysis cells (MEC) were estimated to produce hydrogen at ~\$2 kg per H_2. MECs have a TRL of ~3 and therefore represent a more emerging technology that is capable of achieving a desirable H_2 production cost.

Bridging the gap for photocatalysis can however be achieved through increased investment, collaborative research and development activity with a primary objective being the development of demonstrator plants. While this is ambitious given the prohibitive costs, the recent announcement of the European Hydrogen Bank (EHB) is a leading example of the level of support emerging for renewable hydrogen production. The EHB will offer producers a fixed premium cap of €4.5 per kg H_2 as

Table 5 Various sustainability indicators used in modelling work shown in Fig. 10. Figure reproduced from ref. 87 with permission from Elsevier

Key		
Sustainability benefit	Sustainability risk	Indicators not included in sustainability assessment

People sustainability indicators	Development sustainability indicators	Natural system sustainability indicators	Climate change & emissions sustainability indicators
1. Health & wellbeing	11. Economic performance	26. Ecosystems	33. Climate action
2. Food systems	12. Economic stimulation	27. PM pollutants	34. Standards
3. Land management	13. Infrastructure requirements	28. Oxide pollutants	35. Whole life cycle emissions
4. Decent work	14. Production processes	29. Heavy metals	36. Land & carbon stocks
5. Jobs & skills	15. Mobilisation	30. Water use & efficiency	37. Counterfactual considerations
6. Change in income	16. Distribution	31. Water quality	38. Replaced fuels
7. Equality	17. Innovation	32. Water systems	
8. Strong institutions	18. Supply & system efficiencies		
9. Partnerships	19 Techno-economics		
10. Energy access	20. Bioenergy		
	21. Energy system performances		
	22. Added value products		
	23. Complementing wider sectors		
	24. Land characteristics		
	25. Soil		

a subsidy for a maximum of 10 years in an attempt to establish a renewable hydrogen market. The EU hopes this will bridge the gap between fossil-fuel derived hydrogen and renewable hydrogen as they attempt to reach their ambitious targets of 10 Mt of domestic renewable hydrogen production by 2030. The EHB is the first example of a dedicated financial framework that supports renewable hydrogen generation; moreover, it has been entirely driven by the net zero transition. As that transition progresses, however, more investment and support will be needed which is inclusive of a wider range of renewable technologies, especially for those that support a circular economy such as biohydrogen and photocatalysis. At its core, the EHB is an example of financial support for technologies towards achieving larger scale deployment. It's interesting to note that such an investment was not discussed prior to net zero Emissions laws being passed, which further emphasizes the global energy transition occurring.

The significant advantage of photocatalysis is its ability to contribute towards pollutant removal and waste valorisation while simultaneously generating low-carbon hydrogen. This article has highlighted the excellent work being conducted on photocatalytic valorisation of real-world substrates which demonstrates the potential for the technology. While technology barriers still exist, there is increasing evidence and drivers that suggest photocatalysis is undergoing a transition. In doing so, it has promoted how the technology can contribute towards a circular economy and subsequently support the net zero transition.

5. Current engineering aspects

As mentioned in Section 4, photocatalysis is often described as an "emerging" technology. The majority of photocatalytic research has focused on niche material synthesis and mechanistic investigation using simple model substrates. On the lab scale, photocatalysis is a flourishing research area; however, actual industrial application is somewhat disappointing. In addition to the limited number of literature examples exploring the use of real-world substrates, there are very few examples of photocatalytic technology at industrial level application particularly for energy production. The use of non-sustainable pretreatment steps, basic reactor design that shows little promise for scale up (*e.g.* a test tube), use of niche materials that are not practical for scale up and the use of platinum metal as a co-catalyst highlight some of the limitations for the potential scale up of these processes. In this section we will discuss the main issues in reactor design for photocatalytic scale up and review some of the current technology. Most of the examples in this section involving reactor design focus on environmental remediation and synthesis, rather than energy production.

The main limitations for photocatalytic scale up are photon transfer limitations to the photocatalyst surface and mass

transfer limitations within the reactor. Photons are obtained from either natural sunlight or artificial sources. Natural solar illumination is obviously a highly desirable renewable source of photons; however, it is location dependent and the variability of sunlight is a major drawback. Sunlight reaching the Earth's surface is composed of 55% infra-red (>700 nm), 42–43% visible light (400–700 nm) and 3–5% UV (<400 nm). Because of this there has been a huge drive in research to develop visible light activated photocatalysts. However, the development of more efficient and scalable technologies to be deployed on large scales such as industrial and pilot plants also need to be prioritised over material synthesis.

There has been a number of different technologies developed to enhance and focus light energy and also to reduce loss of light due to scattering or absorption such as solar concentrators and optical fibres. While most of the examples given in this section focus on environmental remediation, there is potential to utilize these designs and applications for photocatalytic energy production.

Solar concentrators are systems that utilize mirrors or lenses to focus a large area of sunlight to a small area, typically used for electricity production.[238] However, they have found use in the harvesting of solar energy to promote light-driven photochemical transformations. A recent paper by Zondag *et al.*[239] describes the development of a luminescent solar concentrator-based photo-microreactor and its application in the solar-driven synthesis of organic molecules. The use of this photo-microreactor allowed for transforming solar energy to a concentrated and wavelength shifted irradiation which matches the absorption characteristics of the photocatalyst. To intensify photochemical reactions, various organic dyes can be introduced to the device to target specific wavelengths through down-conversion of incident light.

Recently Zhang *et al.*[240] described the development of a novel solar energy controllable linear Fresnel photoreactor (LFP) for wastewater treatment using real-world conditions. The reactor was composed of a 6-column mirror set up (Fig. 11 and 12). The reactor was able to track and control solar light and adjust the temperature during a photocatalytic reaction under real weather conditions. For example, under sunny conditions the reactor could maintain the optimal light irradiance and temperature, while under overcast conditions it could provide the highest possible light irradiance and temperature as a control; the performance of LFP was compared to the degradation of common pollutants such as amoxicillin, *E. coli* and rhodamine B, using an inclined plate reactor.

Using the LFP reactor the rhodamine B degradation efficiencies were 2.1, 1.5 and 2.28 fold higher than when using an inclined plate reactor under overcast, slightly overcast and sunny conditions respectively. The degradation of amoxicillin and *E. coli* was also greater using the LFP reactor compared to the inclined plate control reactor under sunny conditions (2 and 1.37 fold greater respectively). LFP could achieve effective adjustment of sunlight by flexibly controlling 6 mirrors according to solar position and weather conditions. The reactor has promising potential as a real sunlight track and control reactor for practical photocatalysis. While this technology has

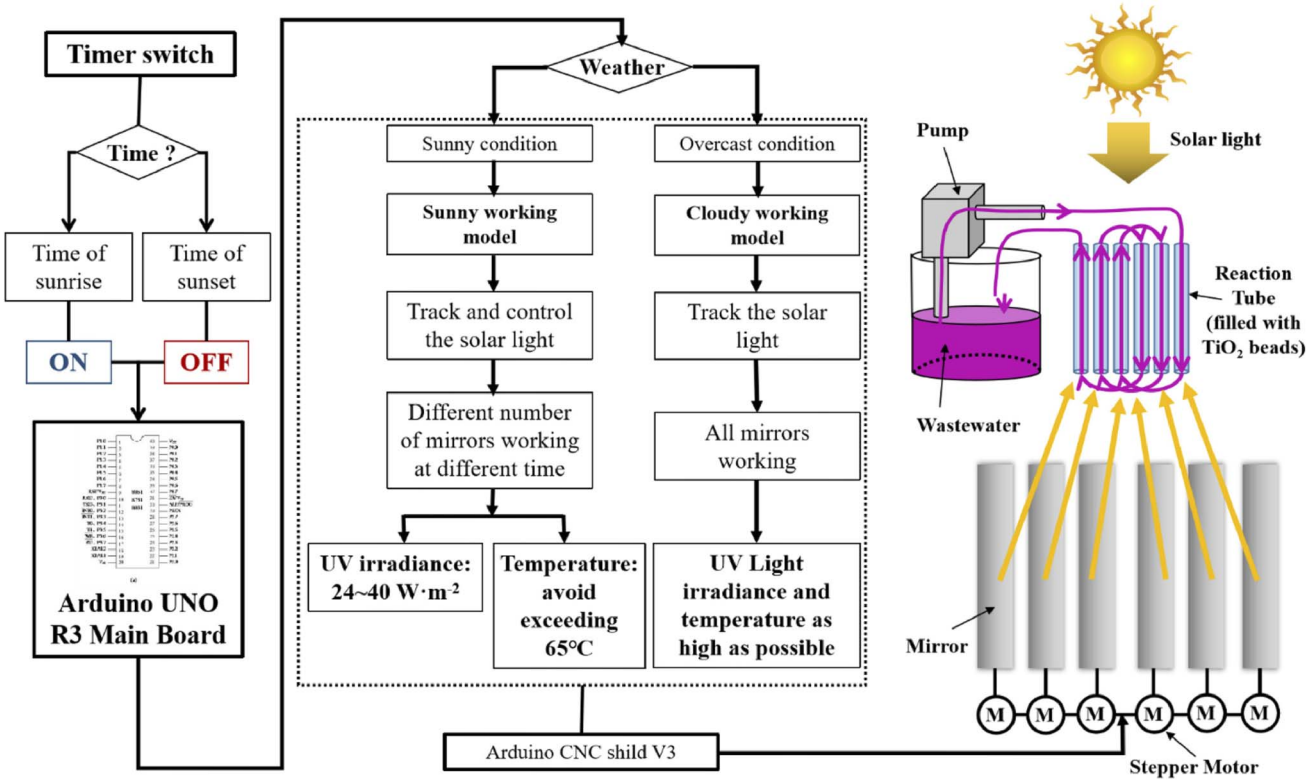

Fig. 11 The flow chart of the LFP control system. Reproduced from ref. 240 with permission from MDPI.

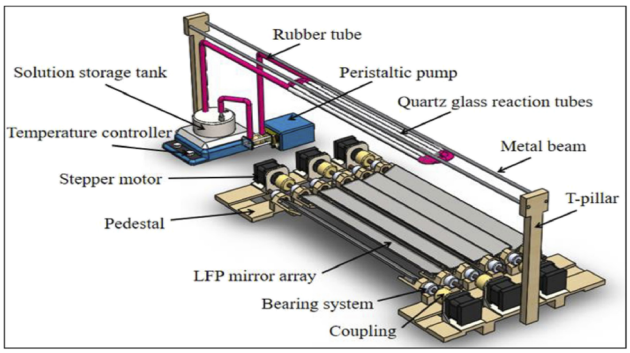

Fig. 12 Blueprint of LFP. Reproduced from ref. 240 with permission from MDPI.

been described for wastewater treatment, it also has the potential for application in photocatalytic energy production.

The use of optical fibres has been employed over the past few decades to reduce the loss of light due to scattering or absorption by the reaction medium. Walko *et al.*[241] have described a scalable optical fibre reactor to produce H_2 photocatalytically from water splitting. The optical fibres were coated with 5% Cu/TiO_2. The photons are transmitted to the catalyst from within the light conducting medium in optical fibres. Under conventional powdered catalyst conditions, it was found that as the quantities of catalyst increased from 50 mg to 1 g the activity reduced exponentially. The scale up in the optical fibre systems was implemented by simply increasing the number of optical fibres. It was found that upon increasing the quantity of optical fibres from 1000 to 50 000, activity also increases from 1 μmol to 120 μmol indicating a linear increase in activity relative to catalyst amount. Hydrogen evolution was more than doubled when the reaction was scaled up to 700 mg of catalyst to 222 μmol. The activity of each system was also tested in highly turbid non-potable water; the optical fibre systems retained *ca.* 70% activity compared to the powdered system which showed complete reduction in activity by 99.99%.

Mass transfer limitations play a vital role in the rate of photochemical reactions. In a homogeneous catalytic system, the catalyst, substrates and products are all in the same phase, hence the effect of mass transfer between phases is negligible. However, in a heterogeneous system, the catalyst is typically in a different phase from the reactants. Consequently, the reaction rate can depend on the mass transfer between or diffusion between these phases.[242] To overcome mass transfer limitations several types of reactors have been developed, including slurry reactors and fixed bed photoreactors. These main types of photoreactor can be further divided into many different reactor types, for example, thin film photoreactors, spinning disk, slurry and monolith, Taylor vortex and fibre optic and membrane photoreactors.[243]

Adams *et al.*[244] developed a novel thin film multi-tubular photoreactor for use with liquid, vapour or gas phase media. The immobilised film design enabled utilization of the full catalyst coating and thus reduced mass transfer limitations by enabling the catalyst and the substrate to be in very close contact. The immobilized catalyst improved the efficiently of the process as a separation step was not required. The design allows for scale up by increasing the length of the glass columns.

O'Neill *et al.*[67] recently compared the inactivation of *E. coli* using a slurry reactor set up and a spinning disk reactor. A spinning disk reactor employs a horizontally aligned rotating disk to create high centrifugal acceleration. When a liquid is fed from the centre onto the reactor the centrifugal forces cause it to spread out into a highly sheared and thin film to improve mass and heat transfer. The thin film also allows higher light penetration. O'Neill *et al.* determined ZnO was the more efficient photocatalyst for *E. coli* removal in both reactor set-ups.

An excellent paper by Khan *et al.*[245] outlines recent advancements in engineering for the design of photoreactors to produce renewable fuels *via* reduction of CO_2. The authors reviewed the pros and cons for typical photoreactors, including slurry, fixed bed and membrane reactors and concluded the fabrication of a hybrid type photoreactor which utilizes positives from each type of reactor would be highly beneficial in the photocatalytic generation of fuels.

The scale up of photochemical reactors presents additional challenges to those associated with the scale up of chemical reactions due to the attenuation effect of photon transport which is directly related to the dimension of reactors. Heterogeneous catalytic systems, which are typically preferred in industry, are challenging as the penetration of light though the catalyst is limited. As mentioned before, due to the lack of examples of reactor design and scale up for energy production we are including examples of the more widely studied area of environmental remediation. However, despite the level of research in this area over the last five decades it has been difficult to find examples of commercialized processes. A recent paper by Mills *et al.*[246] detailed seven companies involved in the commercialization of photocatalytic technology for water treatment, with some listed as having "no obvious products". For those listed with their technologies it proved difficult to find out any additional information. Nevertheless, an industrial scale photocatalytic water purification technology by "Purifics Photo-Cat" which is described as the largest photocatalytic AOP system in the world (Fig. 13) has been developed. The technology uses a TiO_2 slurry based photocatalytic system for water purification.[247]

Imoberdorf *et al.*[248] designed a scaled up multi-annular photocatalytic reactor for the photocatalytic oxidation of

Fig. 13 Reactor technology from Purfics reproduced from ref. 247 with permission from Purifics.

perchloroethylene. In this work the authors investigated six annular photocatalytic wall reactor configurations. For validation purposes a multi-annular reactor with interconnected channels and uniform TiO_2 thickness due to good performance for perchloroethylene oxidation was chosen. A complete reactor model was developed and solved. It was possible to predict reactor behaviour based on this model based on chemical reaction fundamentals, reactor engineering and radiation transport theory. Reactor volume ranged from 633 cm^3 to 2178 cm^3 and photocatalytic active area ranged from 1266 cm^2 to 5208 cm^2 for the 6 reactors investigated in this study.

The scale up of photochemical reactions has also been investigated using continuous flow systems. Typically, the work has focused on photochemical synthesis of organic compounds. For example, Beaver *et al.*[249] developed a high-throughput (>5 kg per day) photochemical flow process to generate >250 kg of the target molecule, cyclobutene. Details of the continuous flow set up can be seen in Fig. 14. The reaction was scaled up from lab scale using a 500 ml volumetric flask, to demo scale that utilized a 50 L flask to production scale that employed a 3000 L stainless steel reactor. A continuous flow set up was found to be significantly safer and more efficient to operate than a batch system at the same scale (Fig. 14 and 15).

Microreactor technology has a wide range of advantages over conventional batch technology and has found use in scaling up of chemical processes. Microreactor technology that utilizes continuous flow operation has enhanced heat and mass transfer rates and large specific surface areas. Microreactors have extremely small dimensions which ensures excellent light irradiation. Throughput can be increased by increasing the number of microreactors. Microreactors also offer increased safety for processing at larger scales compared to batch reactors at a similar scale. Su *et al.*[250] used a numbering up approach in a capillary multiphase flow photoreactor to scale up a photocatalytic oxidation reaction of thiols to disulfides. The yield obtained in the numbered up photoreactors (Fig. 16) was comparable to the yield obtained in a single photo-microreactor device and hence demonstrated the efficiency of the system.

The scale up of any chemical process has its challenges, add in light which is required for photochemical processes and the difficulty significantly increases. Photocatalysis has much potential in a net zero landscape as a renewable technology. As the strive for net zero intensifies it is envisaged that scaling up photochemical processes will ramp up and gain the momentum that is needed to play their part in a net zero future.

6. Overall perspective and future outlook

As with all emerging technologies, it can be challenging to accurately predict the role photocatalysis will play within future energy systems and a stable circular economy. This is further

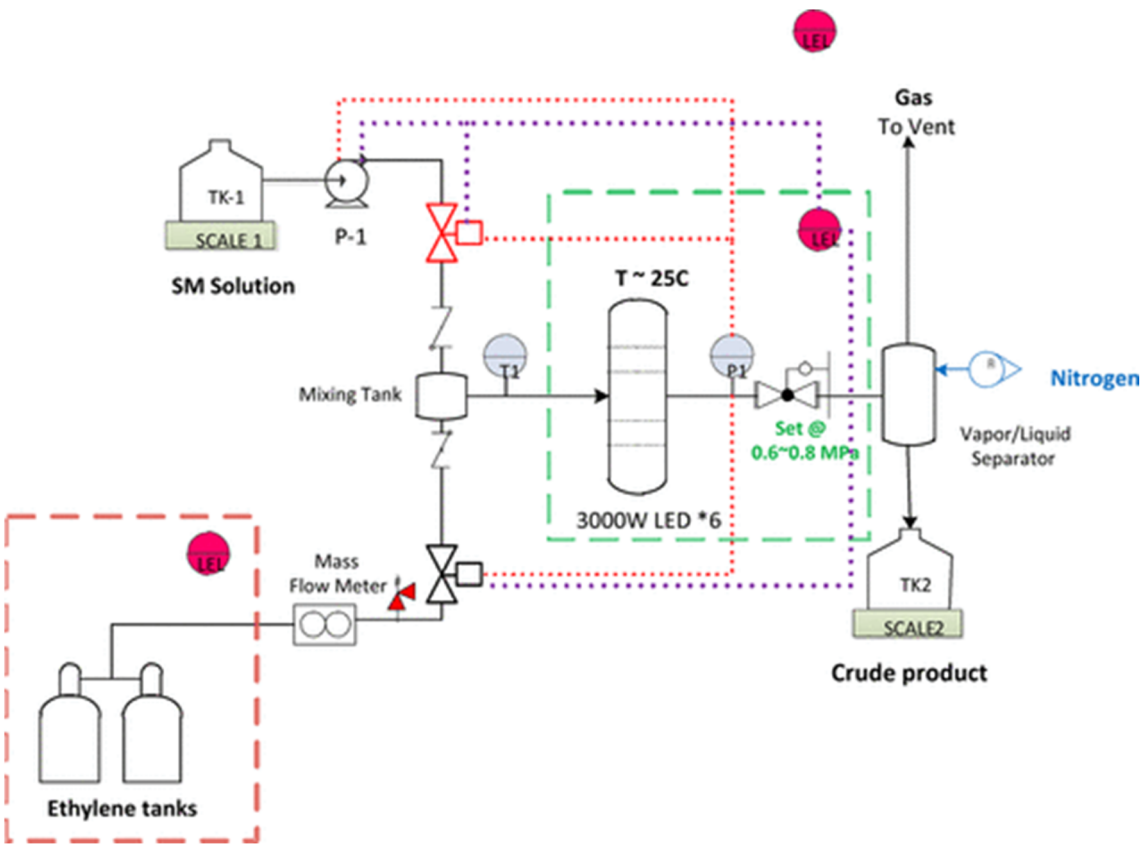

Fig. 14 Modifications to the skid to support safe implementation in the production setting. Reproduced from ref. 249 with permission from American Chemical Society.

Fig. 15 Pictures of the production-scale photochemical skid. Reproduced from ref. 249 with permission from American Chemical Society.

complicated when considering the rapidly changing renewable and sustainable energy landscape associated with the net zero transition. That transition is multi-faceted and complex, and as a result requires solutions which are not just interdisciplinary in nature but capable of achieving an impact across social, economic, environmental and technological platforms. The role and impact of technologies such as photocatalysis will have within that will always be debated, as an emerging technology by its nature requires support to achieve further development and deployment. It's crucial that support facilitates growth, rather than perpetuating a level of academic stagnation or a continued hype cycle which is often associated with trying to develop the 'perfect' material. Moreover, this support must be contextualised in relation to other emerging technologies, as well as those at higher TRLs, which face manufacturing and deployment challenges. Put simply, there may not be enough resources to support all emerging technologies which can contribute towards our low-carbon and net zero targets. It is therefore vital that technologies such as photocatalysis can be evaluated and monitored with a view towards developing a strategy for TRL advancement. This includes assessing the current status, which is frequently done within the literature, and coupling that with identifying research priorities to support growth.

The core advantages of photocatalysis are well known: ambient operating conditions, a low-carbon technology and the generation of highly oxidising reactive species. Leveraging those advantages within future systems is crucial and as demonstrated in this article, can be targeted towards the use of real-world substrates and feedstocks. Therefore, deployment and operation 'beyond the lab' should be a primary objective for photocatalytic technology. Achieving that requires commercial scale availability of new materials, modular reactor design that supports scale up and holistic system level analysis to support industry engagement. In view of the discussion provided in this article, there are key areas which the authors feel should be considered and addressed by the research community in future work. Firstly, availability and sustainability of photocatalytic feedstocks to ensure efficient remediation and valorisation towards valuable products. While photocatalysis can be non-selective towards substrate oxidation, the composition of feedstocks should be carefully considered to maximise the yield of desirable products, while ensuring no harmful by-products are generated. This means photocatalysis should be deployed with appropriate feedstocks, and where necessary pre-treatment should also be used. In addition, it's important that comparisons are made to alternative treatment and conversion processes to ensure feedstocks are correctly coupled with appropriate technologies. This approach can also facilitate integrated and hybrid systems comprised of multiple technologies that promote synergistic effects. This was demonstrated in our previous work to show coupling photocatalysis with acoustic cavitation improved diisobutyl phthalate removal.[251] This approach can also include adopting 'best practices' or 'lessons learned' from other technologies in materials design and reactor engineering *e.g.* achieving stable electron–hole charge separation is a fundamental requirement in photovoltaics and also necessary for photocatalytic hydrogen generation. It should be noted, however, that materials with high charge separation and transfer don't always support ROS generation. Therefore, repurposing materials from other applications or disciplines may not always be viable. In relation to reactor engineering, electrolysers and fuel cells are scalable due to a modular design, which should be adopted by photocatalytic units also. While challenges such as mass transfer limitations and efficient photon delivery will still require consideration, modularity should be a key priority in initial reactor design.

In addition to feedstock considerations, holistic systems analysis is a valuable tool often used to evaluate and compare conversion processes and technologies. It's use with photocatalytic systems, however, is very limited with only a few examples reported in the literature.[252–258] It's important to note that tools such as LCA and TEA are reliant on data availability and for many photocatalytic applications, there is often insufficient data to ensure accurate results from systems analysis are generated. This, however, should not be seen as a reason to disregard such methodologies but instead as an opportunity to assess how additional data can be generated, analysed and interpreted. In the first instance, that can be achieved by utilising metrics that encompass a broader range of operating parameters. Reaction rates (often as a function of irradiation time) along with photonic efficiencies and apparent quantum yields are useful metrics for benchmarking; however, they do not account for other key parameters such as power consumption, environmental impact, cost or scale. Perhaps a key example of this is in relation to environmental remediation and the use of the Electrical Energy per Order (EEO) value which is a tool used for reporting the efficiency of AOPs for organic contamination removal. While this is a standardised metric, which allows for accurate comparison between AOPs, it's rarely reported in the literature for photocatalysis. This reflects the need for a shift and transition within

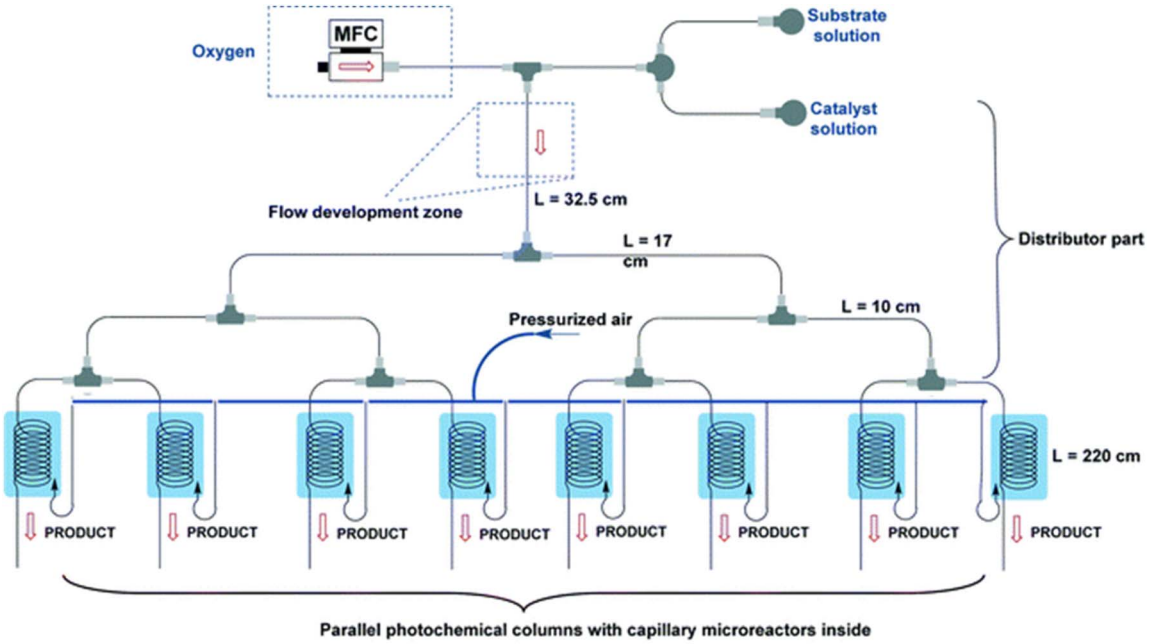

(a)

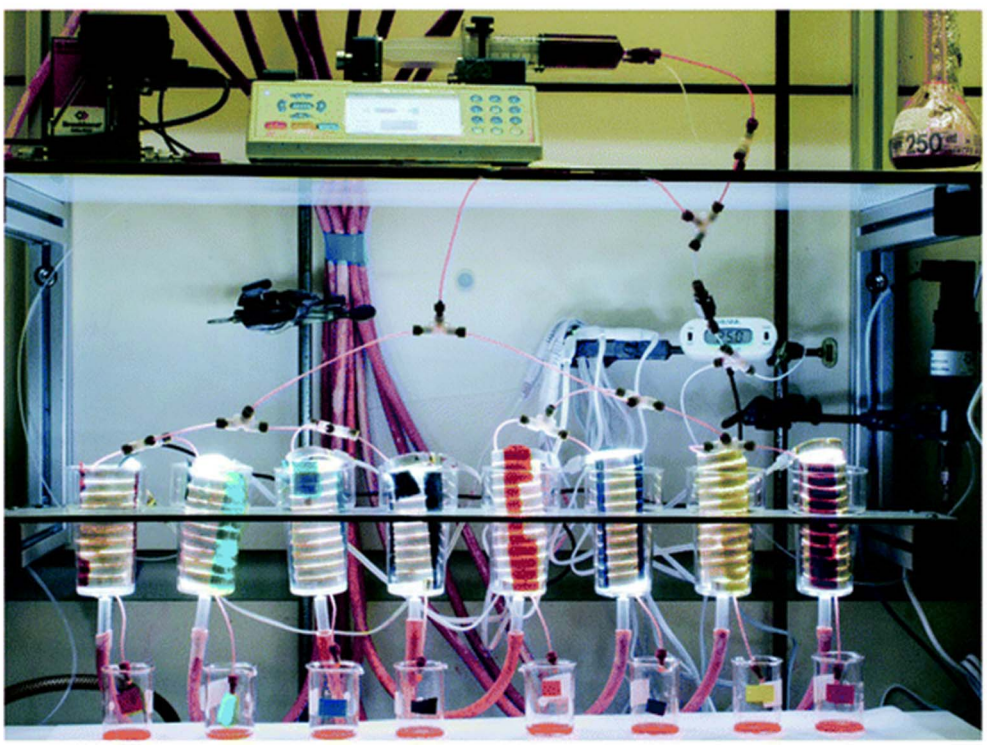

(b)

Fig. 16 (a) Schematic overview of the 8-capillary microreactor system, (b) a picture of the 8-capillary microreactor system with a gas–liquid photocatalytic transformation running. Reproduced from ref. 250 with permission from Chemistry Europe.

photocatalytic (and photoelectrochemical) research towards studies and work that can be assessed across a broader range of metrics to determine the real-world impact.

While limited, it is encouraging to see an increasing number of examples in the literature of LCA and environmental impact assessments being conducted for photocatalysis. Furthermore,

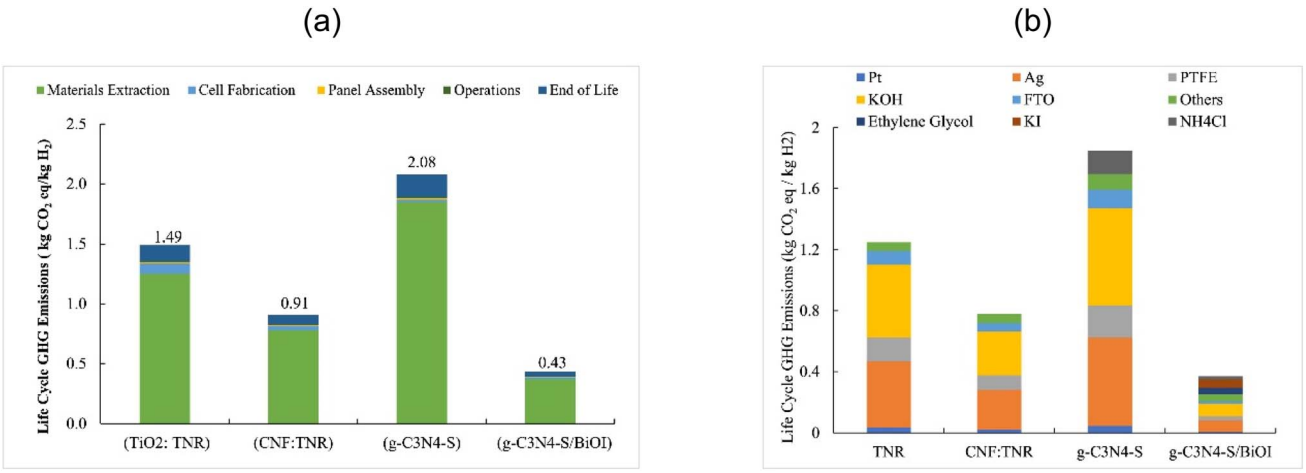

Fig. 17 (a) Life cycle GHG Emissions as a function of catalyst and (b) elemental contribution in material extraction. Reproduced from ref. 257 and with permission from Elsevier.

these examples include both energy production and environmental remediation applications, along with consideration towards key parameters such as the sustainability impact of metal-doping on TiO_2,[255] pilot scale operation[254] and comparison to other conversion technologies.[259] Observing these trends in the literature is important as its evidence of analysing parameters which support photocatalysis technology advancement. Moreover, it addresses key topics such as the sustainability of larger scale operation and the environmental impact of photocatalytic materials development *e.g.* synthesis routes, the use of critical elements, and end-of-life assessments. While these are complex research areas to address for photocatalysis, it's crucial they are seen as priorities and, where possible, incorporated into on-going research. Examples which highlight this in recent literature include the work of Maurya *et al.*[257] in 2023 who performed LCA of earth abundant materials for photocatalytic hydrogen generation. As such materials are often utilised in either synthesis routes or as co-catalysts which facilitate the reduction of protons to H_2, their use and subsequent impact is a crucial parameter when performing systems analysis. This is also a factor when considering catalyst recovery and reuse. The study developed a cradle-to-grave methodology to assess the carbon footprint of TiO_2 and C_3N_4 based photomaterials. The framework encompassed synthesis (*e.g.* material extraction and production), system operation (*e.g.* reactor assembly, H_2 production and storage) and end-of-life (*e.g.* decommissioning and recycling) to generate data which is reflective of full system operation. The data showed for all the catalysts considered (TiO_2 nanorods, fluorine-doped C_3N_4 quantum dots, g-C_3N_4 sheets and C_3N_4/BiOI composites) that materials extraction contributed the largest portion of life cycle GHG emissions based on kg CO_2 eq. per kg H_2. As shown in Fig. 17a, the data ranged from 0.43 for the composite material to 2.08 kg CO_2 eq. per kg H_2 for g-C_3N_4 sheets. In each case, however, materials extraction accounted for >80% of emissions. In addition, the study also demonstrated that KOH and Ag generated the largest GHG emissions based on the elemental contribution for material extraction (Fig. 17b). Interestingly, this data also underpins the importance of catalyst stability over prolonged use, which should encourage the research community to consider catalyst recycling, recovery and any reconditioning steps required to ensure activity is maintained over multiple years. This work and others in the literature highlight the importance of full systems analysis to identify not just strengths and weaknesses in photocatalysis, but also risks and opportunities. It is therefore vital that careful consideration is given towards both materials synthesis routes and reactor design along with end-of-life processes to determine an accurate assessment of environmental impact. In doing so, this will establish a strong rhetoric for supporting the role of photocatalysis as a low-carbon technology capable of contributing towards net zero targets.

7. Conclusion

This review has considered the application of semiconductor photocatalysis to the valorisation of "real-world" wastes as opposed to "model" compounds. From this review a comprehensive range of substrates are clearly amenable to valorisation using this process and there is clear potential to not only process recalcitrant waste materials/chemicals but also simultaneously generate renewable hydrogen and convert the waste to high value chemicals. This clearly demonstrates the applicability of the technology for circular economy applications. While the initial laboratory studies have shown some very promising results, there are several issues and challenges that need to be addressed before this technology will be truly applicable. Firstly, for many of the processes, relatively harsh operating conditions are required utilising strong acids or bases to maximise product yields, and these solvents have their own environmental challenges. Even when the reactions are conducted in strong acids or bases, the product yields are still relatively low, compared to other valorisation processes. For example, the H_2 yields are typically in the μmol g_{cat}^{-1} h^{-1} to mmol g_{cat}^{-1} h^{-1} range. Typically, this means that ml quantities of gas are generated rather than m^3 that would be required

for a commercially practical process. Furthermore, many of the processes also require photocatalysts that have been modified with precious metals such as platinum. This not only increases the cost of the process, but it also has issues with respect to the demand for globally scarce materials. Many of the most effective photocatalysts reported to date also require UV light to activate them. In cases where visible light active materials have been successfully demonstrated, these have mostly involved the use of photocatalysts such as cadmium sulfide which is known to photo-corrode with prolonged irradiation and hence there is a risk of toxic cadmium ions leaching into the environment. As with other semiconductor photocatalytic processes there is a need for cheap, efficient, stable, visible light active photocatalysts if photocatalytic valorisation processes are to be realised on any practical scale. Moving forward there also needs to be significant research effort put into reactor development where the process can process m^3 quantities of the "real-world" wastes and move the technology on from the lab scale as reported in much of the research. While challenges such as mass transfer limitations and efficient photon delivery will still require consideration, modularity should be a key priority in initial reactor design. While there are clearly significant challenges that still need to be addressed if semiconductor photocatalysis is going to be realised as a practical process for valorisation of "real-world" substrates, the research that has been reported in recent years is very promising, having proved the principle and provided a firm foundation for future development.

Data availability

No primary research results, software or code have been included and no new data were generated or analysed as part of this review.

Conflicts of interest

The authors declare no conflict of interest.

Acknowledgements

We would like to acknowledge the funding provided by the Department of Agriculture, Environment and Rural Affairs for supporting this research (contract number 21/R/475 – ValiD – Valorisation of Digestate using Photocatalysis and Hydrodynamic Cavitation).

References

1 https://www.gov.uk/government/speeches/more-than-zero-why-net-zero-alone-wont-save-the-planet-and-what-will, accessed Oct 2023.
2 https://ourworldindata.org/co2-emissions, accessed Oct 2023.
3 https://iea.blob.core.windows.net/assets/91982b4e-26dc-41d5-88b1-4c47ea436882/Coal2022.pdf, accessed Oct 2023.
4 https://www2.bgs.ac.uk/mineralsuk/download/world_statistics/2010s/WMP_2015_2019.pdf. accessed Oct 2023.
5 https://ourworldindata.org/grapher/global-plastics-production, accessed Oct 2023.
6 https://www.fao.org/documents/card/en/c/ca8753en, accessed Oct 2023.
7 https://ourworldindata.org/, accessed Oct 2023.
8 https://ourworldindata.org/biodiversity?insight=wild-mammals-have-declined-by-85-since-the-rise-of-humans#key-insights-on-biodiversity. accessed Oct 2023.
9 https://web.archive.org/web/20080625012113/http://www.virtualcentre.org/en/library/key_pub/longshad/A0701E00.pdf, accessed Oct 2023.
10 J. C. Dodson, P. Dérer, P. Cafaro and F. Götmark, *Sci. Total Environ.*, 2020, **748**, 141346–141356.
11 *Life on the Brink: Environmentalists Confront Overpopulation*, ed. Philip Cafaro and Eileen Crsit, 2012.
12 https://www.un.org/en/global-issues/population, accessed Oct 2023.
13 B. C. O'Neill, B. Liddle, L. Jiang, K. R. Smith, S. Pachauri, M. Dalton and R. Fuchs, *Lancet*, 2012, **380**, 157–164.
14 B. C. O'Neill, M. Dalton, R. Fuchs and K. Zigova, *Proc. Natl. Acad. Sci. U.S.A.*, 2010, **107**, 17521–17526.
15 S. R. Gaffin and B. C. O'Neill, *Popul. Environ.*, 1997, **18**, 389–413.
16 J. C. Dodson, P. Dérer, P. Cafaro and F. Götmark, *Sci. Total Environ.*, 2020, **748**, 141346–141356.
17 J. Bongaarts and B. C. O'Neill, *Science*, 2018, **361**(6403), 650–652.
18 P. D. Habumuremyi and M. Zenawi, *Lancet*, 2012, **380**, 78–80.
19 J. Cleland, A. C-Agudelo, H. Peterson, J. Ross and A. Tsui, *Lancet*, 2012, **380**, 149–156.
20 *Climate Change 2014: Mitigation of Climate Change, Working Group 3 Contribution to the IPCC Fifth Assessment Report*, Cambridge University Press, 2015, accessed October 2023.
21 https://population.un.org/wpp/Methodology. accessed October 2023.
22 https://www.nature.com/articles/461472a.
23 K. Richardson, W. Steffen, W. Lucht, J. Bendtsen, S. E. Cornell, J. F. Donges, M. Druke, I. Fetzer, G. Bala, W. Bloh, G. Feulner, S. Fiedler, D. Gerten, T. Gleeson, M. Hofmann, W. Huiskamp, M. Kummu, C. Mohan, D. Bravo, S. Petri, M. Porkka, S. Rahmstorf, S. Schaphoff, K. Thonicke, A. Tobian, V. Virkki, L. Wang-Erlandsson, L. Weber and J. Rockstrom, *Sci. Adv.*, 2023, **9**, eadh2458.
24 https://ourworldindata.org/contributed-most-global-co2, accessed Jan 2024.
25 https://ourworldindata.org/explorers/population-and-demography, accessed Jan 2024.
26 https://www.statista.com/topics/11239/global-warming/#topicOverview, accessed Jan 2024.
27 https://www.climate.gov/news-features/understanding-climate/climate-change-global-temperature, accessed October 2023.

28 N. R. Golledge, E. D. Keller, N. Gomez, K. Naughten, J. Bernales, L. D. Trusel and T. L. Edwards, *Nature*, 2019, **566**, 65–72.
29 M. Zemp, M. Huss, E. Thibert, N. Eckert, R. McNabb, M. Barandun, H. Machguth, S. U. Nuddbaumer, I. Garner-Roer, L. Thompson, F. Paul, F. Maussion, S. Kutuzov and J. G. Cogley, *Nature*, 2019, **568**, 382–386.
30 E. V. Kennedy, C. T. Perry, P. R. Halloran, R. Iglesias-Prieto, C. H. L. Schonberg, M. Wisshak, A. U. Form, J. P. Carricart-Ganivet, M. Fine, C. M. Eakin and P. J. Mumby, *Curr. Biol.*, 2013, **23**(10), 912–918.
31 N. J. Abram, B. J. Henley, A. S. Gupta, T. J. R. Lippmann, H. Clarke, A. J. Dowdy, J. J. Sharples, R. H. Nolan, T. Zhang, M. J. Wooster, J. B. Wurtzel, K. J. Meissner, A. J. Pittman, A. M. Ukkola, B. P. Murphy, N. J. Tapper and M. M. Boer, *Commun. Earth Environ.*, 2021, **2**, 8.
32 V. Varerla, D. Vlachogiannis, A. Sfetsos, S. Karozis, N. Politi and F. Giroud, *Sustainability*, 2019, **11**(16), 4284–4297.
33 E. Bevacqua, M. I. Vousdoukas, G. Zappa, K. Hodges, T. G. Shepard, D. Maraun, L. Mentaschi and L. Feyen, *Commun. Earth Environ.*, 2020, **1**(47), 2020.
34 M. G. Grillakis, *Sci. Total Environ.*, 2019, **660**(10), 1245–1255.
35 P. H. Raven and D. L. Wagner, *Proc. Natl. Acad. Sci. U.S.A.*, 2021, **118**(2), e2002548117.
36 R. Mukhopadhyay, B. Sarkar, H. S. Jat, R. C. Sharma and N. S. Bolan, *J. Environ. Manag.*, 2021, **280**, 111736–111750.
37 L. C. Stringer, A. Mirzabaev, T. A. Benjaminsen, R. M. B. Harris, M. Jafari, T. K. Lissner, N. Stevens and C. Tirado-von der Pahlen, *One Earth*, 2021, **4**(6), 851–864.
38 **https://unfccc.int/process-and-meetings/the-paris-agreement**. accessed October 2023.
39 UK Government, *The Ten-point Plan for a Green Industrial Revolution*, London, 2020, accessed October 2023.
40 UK Government, *Net Zero Strategy: Build Back Greener*, London, 2021, accessed October 2023.
41 **https://unfccc.int/**, accessed October 2023.
42 **https://climate.mit.edu/explainers/carbon-offsets**, accessed October 2023.
43 S. Fankhauser, S. M. Smith, M. Allen, K. Axelsson, T. Hale, C. Hepburn, J. M. Kendall, R. Khosla, J. Lezaun, E. Mitchell-Larson, M. Obersteiner, L. Rajamani, R. Rickaby, N. Seddon and T. Wetzer, *Nat. Clim. Change*, 2022, **12**, 15–21.
44 **https://www.gov.uk/government/speeches/more-than-zero-why-net-zero-alone-wont-save-the-planet-and-what-will**, accessed Oct 2023.
45 **https://climatechampions.unfccc.int/whats-the-cost-of-net-zero-2/**, accessed Oct 2023.
46 **https://www.gov.uk/government/publications/the-ten-point-plan-for-a-green-industrial-revolution**, accessed Oct 2023.
47 **https://www.gov.uk/government/publications/the-ten-point-plan-for-a-green-industrial-revolution**, accessed Oct 2023.
48 R. Dickson, M. Akhtar, A. Abbas, E. Park and J. Liu, *Green Chem.*, 2022, **24**, 8484–8493.
49 K. de Kleijne, H. de Coninck, R. van Zelm, M. A. J. Huijbregts and S. V. Hanssen, *Sustain. Energy Fuels*, 2022, **6**, 4383–4387.
50 P. Falcone, M. Hiete and A. Sapio, *Curr. Opin. Green Sustainable Chem.*, 2021, **31**, 100506–100514.
51 A. Sartbaeva, V. L. Kuznetsov, S. A. Wells and P. P. Edwards, *Energy Environ. Sci.*, 2008, **1**, 79–85.
52 P. Nikolaidis and A. Poullikkas, *Renew. Sustain. Energy Rev.*, 2017, **67**, 597–611.
53 **https://www.irena.org/Energy-Transition/Technology/Hydrogen**, accessed November 2023.
54 **https://data.bloomberglp.com/professional/sites/24/BNEF-Hydrogen-Economy-Outlook-Key-Messages-30-Mar-2020.pdf**, accessed November 2023.
55 **https://www.pwc.com/gx/en/industries/energy-utilities-resources/future-energy/green-hydrogen-cost.html**, accessed November 2023.
56 **https://www.sgh2energy.com/economics**, accessed November 2023.
57 **https://www.cleanenergywire.org/news/rising-gas-prices-make-green-hydrogen-cheaper-gray-hydrogen**, accessed November 2023.
58 **https://www.gov.uk/government/news/uk-government-launches-plan-for-a-world-leading-hydrogen-economy**, accessed November 2023.
59 R. Taylor, J. Howes, E. Cotton, E. Raphael, P. Kiri, L. Liu, S. Haye, T. Houghton, A. Bauen, M. Altmann and P. Schmidt, *Options for a UK Low Carbon Hydrogen Standard—Final Report*, London, 2021, accessed November 2023.
60 A. C. Lewis, *Environ. Sci.: Atmos.*, 2021, **1**, 201–207.
61 **https://www.gie.eu/blended-hydrogen-for-decarbonisation/**, accessed November 2023.
62 **https://www.gie.eu/blended-hydrogen-for-decarbonisation/**, accessed November 2023.
63 **https://www.rechargenews.com/energy-transition/green-light-given-for-uks-first-hydrogen-blend-in-public-natural-gas-network/2-1-1045075**, accessed November 2023.
64 **https://www.nationalgrid.com/stories/journey-to-net-zero-stories/hygrid-green-hydrogen-blending-project-launches**, accessed November 2023.
65 M. S. Cellek and A. Pinarbasi, *Int. J. Hydrogen Energy*, 2018, **43**(2), 1194–1207.
66 **https://www.cleanegroup.org/wp-content/uploads/Five-Reasons-to-be-Concerned-About-Green-Hydrogen.pdf**, accessed November 2023.
67 S. O'Neill, J. M. C. Robertson, V. Hequet, F. Chazarenc, X. Pang, K. Ralphs, N. Skillen and P. J. K. Robertson, *Ind. Eng. Chem. Res.*, 2023, **62**(45), 18952–18959.
68 J. Scneider, M. Matsuoka, M. Takwuchi, J. Zhanf, Y. Horiuchi, M. Anpo and D. W. Bahnemann, *Chem. Rev.*, 2014, **114**, 9919–9986.
69 *Photocatalysis: Fundamentals and Perspectives*, ed. J. Schneider, D. Bahnemann, J. Ye, G. Li Puma, D. D. Dionysiou, J. Schneider, D. D. Dionysiou, *et al.*, The Royal Society of Chemistry, 2016, pp. P001–P004.

70 K. Nakata and A. Fujishima, *J. Photochem. Photobiol., C*, 2012, **13**, 169–189.
71 D. F. Ollis, E. Pelizzetti, N. Serpone, *Photocatalysis: Fundamentals and Applications*, 1989.
72 M. A. Fox and M. T. Dulay, *Chem. Rev.*, 1993, **93**, 341–357.
73 P. K. J. Robertson, *J. Cleaner Prod.*, 1996, **4**, 203–212.
74 Y. Nosaka and A. Y. Nosaka, *Chem. Rev.*, 2017, **117**, 11302–11336.
75 W. J. McCormick., D. McCrudden, N. Skillen and P. K. J. Robertson, *Appl. Catal., A*, 2023, **660**, 1119201–1119210.
76 D. Chen, Y. Cheng, N. Zhou, P. Chen, Y. Wang, K. Li, S. Huo, P. Cheng, P. Peng, R. Zhang, L. Wang, H. Liu, Y. Liu and R. Ruan, *J. Clean. Prod.*, 2020, **268**, 121725–121740.
77 C. Acar, I. Dincer and G. F. Naterer, *Int. J. Energy Res.*, 2016, **40**, 1449–1473.
78 J. Gong, C. Li and M. R. Wasilewski, *Chem. Soc. Rev.*, 2019, **48**, 1862–1864.
79 J. Bedia, V. Muelas-Ramos, M. Penas-Garzon, A. Gomez-Aviles, J. J. Rodriguez and C. Belver, *Catalysts*, 2019, **9**(1), 52.
80 A. Mamaghani, F. Haghighat and C. Lee, *Appl. Catal. B Environ.*, 2017, **203**, 247–269.
81 D. Robert and A. Laghzizil, *Environ. Sci. Pollut. Res.*, 2023, **30**, 81616–81618.
82 J. Ma, K. Liu, X. Yang, D. Jin, Y. Li, G. Jiao, J. Zhou and R. Sun, *ChemSusChem*, 2021, **14**(22), 4903–4922.
83 V. Rao, T. T. Malu, K. Cheralathan, M. Sakar, S. Pitchaimuthu, V. Rodriguez-Gonzalez, M. M. Kumari and M. V. Shankar, *J. Environ. Manage.*, 2021, **284**, 111983–111998.
84 S. Xu, X. Huang and H. Lu, *Fuel Process. Technol.*, 2024, **255**, 108057–108075.
85 T. Kawai and T. Sakata, *Nature*, 1980, **286**, 474.
86 F. Cherubini, *Energy Convers. Manage.*, 2010, **51**(7), 1412–1421.
87 A. J. Welfle, A. Alemena, M. N. Arshad, S. W. Banks, I. Butnar, K. J. Chong, S. J. G. Cooper, H. Daly, S. G. Freites, F. Gulec, C. Hardacre, r. Holland, L. Lan, C. S. Lee, P. K. J. Roberston, R. Rowe, A. Shepard, N. Skillen, S. Tedesco, P. Thornley, P. V. Barbara, I. Watson, O. S. A. Williams and M. Roder, *Biomass Bioenergy*, 2023, **177**, 1106919–1106938.
88 A. M. Ruppert, K. Weinberg and R. Palkovits, *Angew. Chem., Int. Ed.*, 2012, **51**(11), 2564–2601.
89 K. Tekin, S. Karagoz and S. Bektas, *Renewable Sustainable Energy Rev.*, 2014, **40**, 673–687.
90 C. Xu, R. A. Arancon and J. Labidi, *Chem. Soc. Rev.*, 2014, **43**(22), 7485–7500.
91 J. Wen, B. Xue and F. Xu, *Ind. Crops Prod.*, 2013, **42**, 332–343.
92 F. G. Calvo-Flores and J. A. Dobado, *ChemSusChem*, 2010, **3**(11), 1227–1235.
93 S. Ahmed, T. Warne, E. Smith, H. Goemann, G. Linse, M. G. J. Kedziora, M. Snapp, D. Kraner, K. Roemer, J. H. Haggerty, M. Jarchow, D. Swanson, B. Poulter and P. C. Stoy, *npj Sci. Food.*, 2021, **5**, 9.
94 C. Chen, A. Chaudhary and A. Mathys, *Resour. Conserv. Recycl.*, 2020, **160**, 104912–104924.
95 J. Ruane, A. Sonnino and A. Agostini A, *J. Biomass Bioenergy*, 2010, **34**(10), 1427–1439.
96 H. Bouallagui, H. Lahdheb and E. B. Romdan, *J. Environ. Manage.*, 2009, **90**(5), 1844–1849.
97 L. C. Y. Yongjie and W. Chuangzhi, *Biomass Bioenergy*, 2004, (27), 111–117.
98 P. Weiland, *Appl. Microbiol. Biotechnol.*, 2010, **85**(4), 849–860.
99 H. Liu, G. M. Jiang and H. Y. Zhuang, *Renewable and Sus. Ener. Rev.*, 2008, **12**(5), 1402–1418.
100 L. Lan, H. Daly, R. Sung, F. Tuna, N. Skillen, P. K. J. Roberston, C. Hardacre and X. Fan, *ACS Catal.*, 2023, **13**(13), 8574–8587.
101 A. Speltini, M. Sturini, D. Dondi, E. Annovazzi, F. Maraschi, V. Caratto, A. Profumo and A. Buttafava, *Photochem. Photobiol. Sci.*, 2014, **13**, 1410.
102 C. Chang, N. Skillen, S. Nagarajan, K. Ralphs, J. T. S. Irvine, L. Lawton and P. K. J. Robertson, *Energy Fuels*, 2019, **3**, 1971–1975.
103 A. Caravaca, W. Jones, C. Hardacre and M. Bowker, *Proc. R. Soc. A*, 2016, **472**, 54–75.
104 C. Chen, P. Liu, H. Xia, M. Zhou, J. Zhao, B. K. Sharma and J. Jiang, *Molecules*, 2020, **25**(9), 2109–2123.
105 X. Xu, L. Shi, S. Zhang, Z. Ao, J. Zhang and H. Sun, *Chem. Eng. J.*, 2023, **469**, 143972–143990.
106 C. W. J. Murnaghan, N. Skillen, C. Hardacre, J. Bruce, G. N. Sheldrake and P. K. J. Robertson, *J. Phys.: Energy*, 2021, **3**, 035002.
107 C. W. J. Murnaghan, N. Skillen, B. Hackett, J. Lafferty, P. K. J. Robertson and G. N. Sheldrake, *ACS Sustainable Chem. Eng.*, 2022, **10**(37), 12107–12116.
108 S. Chen, T. Takata and K. Domen, *Nat. Rev. Mater.*, 2017, **2**(10), 1–17.
109 T. Sakata and T. Kawai, *J. Synth. Org. Chem., Jpn.*, 1981, **39**(7), 589–602.
110 A. Speltini, M. Sturini and D. Dondi, *Photochem. Photobiol. Sci.*, 2014, **13**(10), 1410–1419.
111 M. Yasuda, R. Kurogi and H. Tsumagari, *Energies*, 2014, **7**(7), 4087–4097.
112 Y. Zhou, X. Ye and D. Lin, *Int. J. Energy Res.*, 2020, **44**(6), 4616–4628.
113 W. Yuan, Z. Gong and G. Wang, *Biores. Tech.*, 2018, **265**, 464–470.
114 A. Caravaca, W. Jones and C. Hardacre, *Proc. R. Soc. A*, 2016, **472**(2191), 20160054.
115 R. Jaswal, R. Shende, A. Shende and W. Nan, *Int. J. Hydrogen Energy*, 2017, **42**(5), 2839–2848.
116 H. Nagakawa and M. Nagata, *Adv. Mater. Interfac.*, 2022, **9**(2), 2101581.
117 H. Nagakawa and M. Nagata, *ACS Appl. Energy Mater.*, 2020, **4**(2), 1059–1062.
118 H. Kasap, D. A. Achilleos and A. Huang, *J. Am. Chem. Soc.*, 2018, **140**(37), 11604–11607.
119 M. Uğurlu, A. Gürses and Ç. Doğar, *J. Environ. Manag.*, 2008, **87**(3), 20–428.

120 D. Pokhrel and T. Viraraghavan, *Sci. Total Environ.*, 2004, **333**(1–3), 37–58.
121 J. W. Owens, S. M. Wanson and D. A. Birkholz, *Chemosphere*, 1994, **29**(1), 89–109.
122 K. K. Vass, M. K. Mukhopadhyay and K. Mitra, *Environ. Ecol.*, 1996, **14**(4), 895–897.
123 A. Schnell, P. V. Hodson and P. Steel, *Water Res.*, 2000, **34**(2), 501–509.
124 P. Lindstrom-Seppa, S. Huuskonen and S. Kotelevtsev, *Mar. Environ. Res.*, 1998, **46**(1), 273–278.
125 H. Leppänen and A. Oikari, *Environ. Toxicol. Chem.*, 1999, **18**(7), 1498–1505.
126 N. Zhong, X. Yu and H. Zhao, *Catalysts*, 2022, **12**(8), 819.
127 J. Zou, G. Zhang and X. Xu, *Appl. Catal., A*, 2018, **563**, 73–79.
128 M. P. Shah, *Advanced Oxidation Processes for Effluent Treatment Plants*, Elsevier, 2020.
129 R. K. Goswami, K. Agrawal and P. Verma, *J. Basic Microbiol.*, 2022, **62**(3–4), 279–295.
130 A. Speltini, F. Gualco and F. Maraschi, *Int. J. Hydrogen Energy*, 2019, **44**(8), 4072–4078.
131 A. Speltini, M. Sturini and D. Dondi, *Photochem. Photobiol. Sci.*, 2014, **13**(10), 1410–1419.
132 S. T. Nguyen, P. R. D. Murray and R. R. Knowles, *ACS Catal.*, 2020, **10**(1), 800–805.
133 L. Lan, H. Daly and R. Sung, *ACS Catal.*, 2023, **13**, 8574–8587.
134 S. Xu, P. Zhou and Z. Zhang, *J. Am. Chem. Soc.*, 2017, **139**(41), 14775–14782.
135 P. Zhou and Z. Zhang, *Catal. Sci. Technol.*, 2016, **6**(11), 3694–3712.
136 H. Priefert, J. Rabenhorst and A. Steinbüchel, *Appl. Microbiol. Biotechnol.*, 2001, **56**(3), 296–314.
137 E. Greenbaum, C. V. Tevault and C. Y. Ma, *Energy Fuels*, 1995, **9**(1), 163–167.
138 S. T. Nguyen, P. R. D. Murray and R. R. Knowles, *ACS Catal.*, 2020, **10**(1), 800–805.
139 X. Wu, X. Fan and S. Xie, *Nat. Catal.*, 2018, **1**(10), 772–780.
140 Y. Lu, X. Wei and Z. Wen, *Fuel Process. Technol.*, 2014, **117**, 8–16.
141 **https://www.bpf.co.uk/industry/Benefits_of_Plastics.aspx**, accessed November 2023.
142 **https://www.wwf.org.au/news/blogs/the-lifecycle-of-plastics**, accessed November 2023.
143 **https://www.oecd.org/environment/plastic-pollution-is-growing-relentlessly-as-waste-management-and-recycling-fall-short.htm**, accessed November 2023.
144 D. C. Ashworth, P. Elliot and M. B. Toledano, *Environ. Int.*, 2014, **69**, 120.
145 R. Geyer, J. R. Jambeck and K. L. Law, *Sci. Adv.*, 2017, **3**(No), e1700782.
146 J. M. Garcia and M. L. Robertson, *Science*, 2017, **358**, 870–872.
147 S. B. Borrelle, J. Ringma, K. L. Law, C. C. Monnahan, L. Lebreton, A. McGivern, E. Murphy, J. Jambeck, G. H. Leonard and M. A. Hilleary, *Science*, 2020, **369**(6510), 1515–1518.
148 C. J. Rhodes, *Sci. Prog.*, 2018, **101**(3), 207–260.
149 L. Lebreton, B. Slat, F. Ferrari, B. Sainte-Rose, J. Aitken, R. Marthouse, S. Hajbane, S. Cunsolo, A. Schwarz and A. Levivier, *Sci. Rep.*, 2018, **8**, 46666.
150 **https://theoceancleanup.com/updates/the-exponential-increase-of-the-great-pacific-garbage-patch/**, accessed November 2023.
151 A. Ragusa, A. Svelatoa, C. Santacroce, P. Catalano, V. Notarstefano, O. Carnevali, F. Papa, M. Antonio, R. F. Baiocco, S. Draghi, E. D'Amore, D. Rinaldo, M. Matta and E. Giorgini, *Environ. Int.*, 2021, **146**, 106274–106282.
152 G. Kutralam-Muniasamy, V. C. Shruti, F. Perez-Guevara and P. D. Roy, *Sci. Total Environ.*, 2023, **856**, 156164–156175.
153 H. A. Leslie, M. J. M. van Velzen, S. H. Brandsma, A. D. Vethaak, J. J. Garcia-Vallejo and M. H. Lamoree, *Environ. Int.*, 2022, **163**, 107199–107207.
154 P. Schwabl, S. Koppel, P. Konigsofer, T. Bucsics, M. Trauner, T. Reilberger and B. Liebmann, *Ann. Intern. Med.*, 2019, **171**(7), 453–457.
155 N. Zhang, Y. B. Li, H. R. He, J. F. Zhang and G. S. Ma, *Sci. Total Environ.*, 2021, **767**, 144345–144352.
156 Y. S. Ibrahim, S. T. Anuar, A. A. Azmi, W. M. A. Khalik, S. Lehata, S. R. H. D. Ismail, Z. F. Ma, A. Dzulkarnaen, Z. Zakaria, N. Mustaffa, S. E. T. Sharif and Y. Y. Lee, *JGH Open*, 2020, **5**(1), 116–121.
157 L. C. Jenner, J. M. Rotchell, R. T. Bennett, M. Cowen, V. Tentzeris and l. R. Sadofsky, *Sci. Total Environ.*, 2022, **831**, 154907–154917.
158 G. Sorci and C. Loiseau, *EBioMedicine*, 2022, **82**, 1041911–1041913.
159 **https://www.theguardian.com/environment/2020/aug/17/microplastic-particles-discovered-in-human-organs**, accessed November 2023.
160 M. Prust, J. Meijer and R. H. S. Westerink, *Part. Fibre Toxicol.*, 2020, **17**, 24.
161 M. Carbery, W. O'Connor and P. Thavamani, *Environ. Int.*, 2018, **115**, 400–409.
162 D. Eerkes-Medrano, H. A. Leslie and B. Quinn, *Curr. Opin Environ. Sci. Health*, 2019, **7**, 69–75.
163 J. Kwon, J. Kim, T. D. Pham, A. Tarafdar, S. Hong, S. Chun, S. Lee, D. Kang, J. Kim and S. Kim, *Int. J. Environ. Res. Publ. Health*, 2020, **17**, 6710.
164 C. Bai, L. Liu, Y. Hu, E. Y. Zeng and Y. Guo, *Sci. Total Environ.*, 2022, **806**, 150263.
165 C. Rubio-Armendáriz, S. Alejandro-Vega, S. Paz-Montelongo, Á. J. Gutiérrez-Fernández, C. J. Carrascosa-Iruzubieta and A. Hardisson-de la Torr, *Int. J. Environ. Res. Public Health*, 2022, **19**, 1174–1188.
166 O. G. Conti, M. Ferrante, M. Banni, C. Favara, I. Nicolosi, A. Cristaldi, M. Fiore and P. Zuccarello, *Environ. Res.*, 2020, **187**, 109677.
167 G. utralam-Muniasamy, F. Pérez-Guevara, I. Elizalde-Martínez and V. C. Shruti, *Sci. Total Environ.*, 2020, **714**, 6823.
168 Y. Huang, J. Chapman, Y. Deng and D. Cozzolino, *Food Control*, 2020, **113**, 107187.

169 V. C. Hruti, F. Pérez-Guevara, I. Elizalde-Martínez and G. Kutralam-Muniasamy, *Sci. Total Environ.*, 2020, **726**, 138580.
170 C. Campanale, S. Galafassi, I. Savino, C. Massarelli, V. Ancona, P. Volta and V. F. Uricchio, *Sci. Total Environ.*, 2022, **805**, 150431.
171 K. S. Basri, A. Daud, R. D. P. Astuti and K. Basri, *Maced. J. Med. Sci.*, 2021, **9**, 275–280.
172 P. Soni and S. Joseph, *Pharma Technol. J.*, 2021, **45**(1), 40–43.
173 D. Materić, *Environ. Pollut.*, 2021, **288**, 117697.
174 J. Brahney, M. Hallerud, M. Hahneberger and S. Sujumaran, *Science*, 2020, **368**(6496), 1257–1260.
175 M. Aeschlimann, G. Li, Z. A. Kanji and D. M. Mitrano, *Nat. Geosci.*, 2022, **15**, 967–975.
176 G. Ren, H. Han, Y. Wang, S. Liu, J. Zhao, X. Meng and Z. Li, *Nanomaterials*, 2021, **11**(7), 1804–1826.
177 A. Kushniarou, G. Navarro and S. Navarro, *Chemosphere*, 2019, **214**, 839–845.
178 N. Vela, M. Calín and M. J. Yáñez-Gascón, *J. Photochem. Photobiol., A*, 2018, **353**, 271–278.
179 H. D. Burrows, L. M. Canle, J. A. Santaballa and S. Steenken, *J. Photochem. Photobiol. B Biol.*, 2002, **67**, 71–108.
180 W. J. McCormick, D. McCrudden, N. Skillen and P. K. J. Robertson, *Appl. Catal., A*, 2023, **660**, 1119201–1119210.
181 H. N. Haslina, N. M. Hafiz and R. M Syamim, *MATEC Web Conf.*, 2016, **47**, 1–6.
182 W. Li, Y. Shi and L. Gao, *Sci. Total Environ.*, 2013, **445–446**, 306–313.
183 A. R. Khataee and M. B. Kasiri, *J. Mol. Catal. A:Chem.*, 2010, **328**, 8–26.
184 J. Šíma and P. Hasal, *Chem. Eng. Trans.*, 2013, **32**, 79–84.
185 E. A. Emam and N. A. K. Aboul-Gheit, *Energy Sources, Part A*, 2014, **36**, 1123–1133.
186 C. J. Pestana, J. Hui, D. Camacho-Munoz, C. Edwards, P. K. J. Roberston, J. T. S. Irvine and L. A. Lawton, *Chemosphere*, 2023, **310**, 136828–136838.
187 X. Pang, V. P. Sarvothaman, N. Skillen, Z. Wang, D. W. Rooney, V. V. Ranade and P. K. J. Roberston, *Chem. Eng. J.*, 2022, 136494–136506.
188 Z. Ouyang, Y. Yang, C. Zhang, S. Zhu, L. Qin, W. Wang, D. He, Y. Zhou, H. Luo and F. Qin, *J. Mater. Chem. A*, 2021, **9**, 13402.
189 Q. Y. Lee and H. Li, *Micromachines*, 2021, **12**, 907.
190 M. Malhotra, L. Pisharody, A. V. Karim and S. Krishnan, *Mater. Res. Found.*, 2021, **99**, 163.
191 Q. Xu, Q. S. Huang, T. Y. Luo, R. L. Wu, W. Wei and B. J. Ni, *Chem. Eng. J.*, 2021, **416**, 129123.
192 P. Ebrahimbabaie, K. Yousefi and J. Pichtel, *Sci. Total Environ.*, 2022, **806**, 150603.
193 S. Horikoshi, N. Serpone, Y. Hisamatsu and H. Hidaka, *Environ. Sci. Technol.*, 1998, **32**, 4010–4016.
194 B. Ohtani, S. Adzuma, S. Nishimoto and T. Kagiya, *Polym. Degrad. Stab.*, 1992, **35**, 53–60.
195 T. S. Tofa, K. L. Kunjali, S. Paul and J. Dutta, *Environ. Chem. Lett.*, 2019, **17**, 1341–1346.
196 D. Castilla-Caballero, O. Sadak, J. Martínez-Díaz, V. Martínez-Castro, J. Colina-Márquez, F. Machuca-Martínez, A. Hernandez-Ramirez, S. Vazquez-Rodriguez and S. Gunasekaran, *Mater. Sci. Semicond. Process.*, 2022, **149**, 106890–106911.
197 A. Chen, M. Yang, S. Wang and Q. Qian, *Frontal Nanotechnol.*, 2021, **3**, 723120.
198 Z. Ouyang, Y. Yang, C. Zhnag, S. Zhu, L. Qin, W. Wang, D. He, Y. Zhou, H. Luo and F. Qin, *J. Mater. Chem. A*, 2021, **9**, 13402–13441.
199 T. Kawai and T. Sakata, *Chem. Lett.*, 1981, **10**(1), 81–84.
200 T. Uekert, M. F. Kuehnel, D. W. Wakerley and E. Reisner, *Energy Environ. Sci.*, 2018, **11**, 2853–2857.
201 T. Uekert, H. Kasap and E. Reisner, *J. Am. Chem. Soc.*, 2019, **141**(38), 15201–15210.
202 T. Li, A. Vijeta, C. Casadevall, A. S. Gentleman, T. Euser and E. Reisner, *ACS Catal.*, 2022, **12**(14), 8155–8163.
203 Y. Li, S. Wan, L. Gao, Y. Lu, L. Wang and K. Zhang, *Sol. RRL*, 2020, **5**, 2000427–2000434.
204 M. Du, Y. Zhang, S. Kang, X. Guo, Y. Ma, M. Xing, Y. Zhu, Y. Chai and B. Qiu, *ACS Catal.*, 2022, **12**(20), 12823–12832.
205 X. Jiao, K. Zheng, Q. Chen, X. Li, Y. Li, W. Shao, J. Xu, J. Zhu, Y. Pan, Y. Sun and Y. Xie, *Angew. Chem., Int. Ed.*, 2020, **132**, 15627–15631.
206 S. Linley and E. Reisner, *Adv. Sci.*, 2023, **10**, 2207314–2207325.
207 S. Hanchang, Encyclopedia of life support systems, *Point Sources of Pollution: Local Effects and Control*, 2009, vol. 1, pp. 191–203.
208 S. M. Abdelbasir and A. E. Shalan, *Korean J. Chem. Eng.*, 2019, **36**, 1209–1225.
209 R. B. Geerdink, R. S. van den Hurk and O. J. Epema, *Anal. Chim. Acta*, 2017, **961**, 1–11.
210 W. H. Saputera, A. F. Amri, R. Daiyan and D. Sasongko, *Materials*, 2021, **14**(11), 2846–2881.
211 A. Moses, J. Komandur, D. Maarisetty, P. Mohapatra and S. S. Baral, *Biomass Convers. Biorefin.*, 2022, **14**, 3135–3159.
212 S. Li, S. Zhao, S. Yan, Y. Qiu, C. Song, Y. Li and Y. Kitamura, *Chin. J. Chem. Eng.*, 2019, **27**(12), 2845–2856.
213 S. Varjani, P. Rakholiya, T. Shindhal, A. V. Shah and H. H. Ngo, *J. Water Process Eng.*, 2021, **39**, 101734.
214 S. S. Tak, O. Shetye, O. Muley, H. Jaiswal and S. N. Malik, *Int. J. Hydrogen Energy*, 2022, **47**(88), 37282–37301.
215 N. Skillen, H. Daly, L. Lan, M. Aljohani, C. W. J. Murnaghan, X. Fan, C. Hardacre, G. N. Sheldrake and P. K. J. Robertson, *Top. Curr. Chem.*, 2022, **380**(5), 33.
216 M. Imizcoz and A. V. Puga, *Catalysts*, 2019, **9**(7), 584.
217 S. Y. Arzate Salgado, R. M. Ramírez Zamora, R. Zanella, J. Peral, S. Malato and M. I. Maldonado, *Int. J. Hydrogen Energy*, 2016, **41**(28), 11933–11940.
218 M. I. Badawy, M. Y. Ghaly and M. E. M. Ali, *Desalination*, 2011, **267**(2–3), 250–255.
219 A. Speltini, M. Sturini, F. Maraschi, D. Dondi, G. Fisogni, E. Annovazzi, A. Profumo and A. Buttafava, *Int. J. Hydrogen Energy*, 2015, **40**(12), 4303–4310.
220 A. E. H. Machado, J. A. de Miranda, R. F. de Freitas, E. T. F. Duarte, L. F. Ferreira, Y. D. Albuquerque,

R. Ruggiero, C. Sattler and L. de Oliveira, *J. Photochem. Photobiol., A*, 2003, **155**(1–3), 231–241.
221 W. Zhang, Y. Li, C. Wang, P. Wang, Q. Wang and D. Wang, *Water Res.*, 2013, **47**(9), 3173–3182.
222 W. Cheng, N. Singh, J. A. Maciá-Agulló, G. D. Stucky, E. W. McFarland and J. Baltrusaitis, *Int. J. Hydrogen Energy*, 2012, **37**, 13304–13313.
223 S. N. Khan, Z. Yang, W. Dong and M. Zhao, *Sustain. Energy Fuels*, 2022, **6**, 4357–4374.
224 G. Pipitone, G. Zoppi, R. Pirone and S. Bensaid, *Int. J. Hydrogen Energy*, 2022, **47**, 151–180.
225 A. Chanthakett, M. T. Arif, M. M. K. Khan and A. M. T. Oo, in *Bioenergy Resources and Technologies*, 2021, pp. 219–247.
226 I. Michielsen, *Plasma Catalysis: Study of Packing Materials on CO_2 Reforming in a DBD Reactor*, University of Antwerp, 2019.
227 S. N. Khan, Z. Yang, W. Dong and M. Zhao, *Sustain. Energy Fuels*, 2022, **6**, 4357–4374.
228 C. Dolle, N. Neha and C. Coutanceau, *Curr. Opin. Electrochem.*, 2022, **31**, 100841–100847.
229 L. Bromberg, D. R. Cohn and A. Rabinovich, *Int. J. Hydrogen Energy*, 1997, **22**, 83–94.
230 S. K. Loeb, P. J. J. Alvarez, P. J. J. Alvarez, J. A. Brame, E. L. Cates, W. Choi, J. Crittenden, D. D. Dionysiou, Q. Li, G. Li-Puma, X. Quan, D. L. Sedlak, T. D. Waite, P. Westerhoff and J. H. Kim, *Environ. Sci. Technol.*, 2019, **53**(6), 2937–2947.
231 S. K. Loeb, P. J. J. Alvarez, J. A. Brame, E. L. Cates, W. Choi, J. Crittenden, D. D. Dionysiou, Q. Li, G. Li-Puma, X. Quan, D. L. Sedlak, T. David Waite, P. Westerhoff and J.-H. Kim, *Environ. Sci. Technol.*, 2019, **53**(6), 2937–2947.
232 N. Skillen, H. Daly, L. Lan, M. Aljohani, C. W. J. Murnaghan, X. Fan, C. Hardacre, G. N. Sheldrake and P. K. J. Robertson, *Top. Curr. Chem.*, 2022, **380**, 33.
233 M. Rumayor, J. Corredor, M. J. Rivero and I. Ortiz, *J. Clean. Prod.*, 2022, **336**, 130430–130441.
234 D. Bahnemann, P. K. J. Roberston, C. Wang, W. Choi, H. Daly, M. Danish, H. de Lasa, S. Escobedo, C. Hardacre, T. H. Jeon, B. Kim, H. Kisch, W. Li, M. Long, M. Muneerm, N. Skillen and J. Zhnag, *J. Phys.: Energy*, 2023, **5**, 012004–012032.
235 H. Nishiyama, T. Yamda, M. Nakabayashi, Y. Maehara, M. Yamaguchi, Y. Kuromiya, Y. Nagatsuma, H. Tokudome, S. Akiyama, T. Watanabe, R. Narushima, S. Okunaka, N. Shibata, T. Takate, T. Hisatomi and K. Domen, *Nature*, 2021, **598**, 304–318.
236 D. Bahnemann, P. K. J. Robertson, C. Wang, W. Choi, H. Daly, M. Danish, H. Lasa, S. Escobedo, C. Hardacre, T. Jeon, B. Kim, H. Kosch, W. Li, M. Long, M. Muneer, N. Skillen and J. Zhang, *J. Phys.: Energy*, 2023, **5**, 012004.
237 P. Ganeshan, V. S. Vigneswaran, S. C. Gowd, D. Kondusamy, C. S. Kuma, N. Kirshnanmoorthy, D. Kumar, A. Juneja, B. Paramasivan, N. N. Raju, K. Rajendran and A. Pugazhendhi, *Fuel*, 2023, **341**, 127601–127619.
238 C. Zhan, N. Li and G. An, *Energies*, 2024, **17**(2), 463.
239 S. D. A. Zondag, T. M. Masson, M. G. Debije and T. Noel, *Photochem. Photobiol. Sci.*, 2022, **21**, 705–717.
240 C. Zhang, N. Liu, J. Ming, A. Sharma, Q. Ma, Z. Liu, G. Chen and Y. Yang, *Water Res.*, 2022, **208**, 117880.
241 P. S. Walko and R. N. Devi, *Int. J. Hydrogen Energy*, 2023, **48**, 17086–17096.
242 R. Klaewkla, M. Arend and W. F. Hoelderich, A Review of Mass Transfer Controlling the Reaction Rate in *Heterogeneous Catalytic Systems, Mass Transfer – Advanced Aspects*, ed. H. Nakajima, InTech, 2011, ISBN: 978-953-307-636-2.
243 C. McCullagh, N. Skillen, M. Adams and P. K. J. Robertson, *J. Chem. Technol. Biotechnol.*, 2011, **86**, 1002–1017.
244 M. Adams, N. Skillen, C. McCullagh and P. K. J. Robertson, *Appl. Catal. B Environ.*, 2013, **130–131**, 99–105.
245 A. A. Khan and M. Tahir, *J. CO_2 Util.*, 2019, **29**, 205–239.
246 A. Mills and S. K. Lee, *J. Photochem. Photobiol., A*, 2002, **152**, 233–247.
247 **https://www.purifics.com/photo-cat**, accessed June 2024.
248 G. E. Imoberdorf, A. E. Cassano, H. A. Irazoqui and O. M. Alfano, *Catal. Today*, 2007, **129**, 118–126.
249 M. G. Beaver, E. Zhang, S. Zheng, B. Wang, J. Lu, J. Tao, M. Gonzalez, S. Jones and J. S. Tedrow, *Org. Process Res. Dev.*, 2020, **24**(10), 2139–2146.
250 Y. Su, N. J. W. Straathof, V. Hessel and T. Noel, *Chem.–Eur. J.*, 2014, **20**, 10562–10589.
251 X. Pang, V. P. Sarvothaman, N. Skillen, Z. Wang, D. W. Rooney, V. V. Ranade and P. K. J. Robertson, *Chem. Eng. J.*, 2022, **444**, 136494–136506.
252 J. F. J. R. Pesqueira, M. F. R. Pereira and A. M. T. Silva, *J. Clean. Prod.*, 2024, **444**, 140845–140855.
253 M. A. Tony and M. M. Eltabey, *Appl. Water Sci.*, 2022, **12**, 21–38.
254 I. Munoz, J. Peral, J. A. Ayllon, S. Malato, P. Passarinho and X. Domenech, *Water Res.*, 2006, **40**(19), 3533–3540.
255 S. Fernandes, J. C. G. Esteves da Silva and L. Pinto da Silva, *Material*, 2020, **25**(13), 1487–1501.
256 M. Rumayor, J. Corredor, M. J. Rivero and I. Ortiz, *J. Clean. Prod.*, 2022, **336**(15), 130430–130441.
257 J. Maurya, E. Gemechu and A. Kumar, *Int. J. Hydrogen Energy*, 2023, **48**(52), 20077–20095.
258 A. Quintavalla, D. Carboni and M. Lombardo, *ChemCatChem*, 2024, **16**, e202301225.
259 J. Dufour, D. P. Serrano, J. L. Galvez, A. Gonzalez, E. Soria and J. L. G. Fierro, *Int. J. Hydrogen Energy*, 2012, **37**(2), 1173–1183.